AJSE

# American Journal of Science & Engineering

Volume 1 Issue 4

December 2020

American Journal of Science & Engineering (AJSE)
Society for Makers, Artists, Researchers and Technologists (SMART)
6408 Elizabeth Ave SE, Auburn 98092, Washington, USA
ISSN: 2687-9530 (Print) and 2687-9581 (Online)

# Editor-in-Chief

## Dr. Chuck Easttom

Capitol Technology University, USA

**Research Interest:** Cryptography, Cyber Warfare, Engineering Processes and Digital Forensics.

Dr. Chuck Easttom is the author of 29 books, including several on computer security, forensics, and cryptography. He has also authored scientific papers on digital forensics, cyber warfare, cryptography, and applied mathematics. He is an inventor with 20 computer science patents. He holds a Doctor of Science (D.Sc.) in cyber security (dissertation topic: a study of lattice-based algorithms for post quantum cryptography) and a Doctor of Philosophy (Ph.D.) in Technology focused on bioengineering and nanotechnology. Dissertation topic is "The effects of nonlinear dynamics on nanotechnology and bioengineering" as well as three master's degrees (one in applied computer science and one in systems engineering). He also has 55 industry certifications (CISSP, CEH, etc.) He has been active in the IEEE Systems and Software Engineering Standards Committee in the 2675 DevOps group and the P2731 Brain Computer Interface standards group, as well as a reviewer for IEEE Open Access. He is a Distinguished Speaker of the ACM and senior member of the ACM as well as a Distinguished Visitor of the IEEE and an IEEE Senior Member. Dr. Easttom is an adjunct lecturer for Georgetown University teaching graduate cyber security courses in their Master of Professional Studies in Applied Intelligence program and an adjunct professor for the University of Dallas teaching digital forensics.

**From the Editor's Desk:**

**A thought about scientific rigor on research:** As scientists, we must always be striving to produce not just more research, but better quality research. A researcher should be his or her own harshest critic. Look at your own work with a skeptical eye. Could you provide clearer data? Are your references adequate and current? Is your statistical analysis appropriate and robust? Our goal as scientists is not merely to publish research, but to produce research that is truly impactful. By constantly striving to improve the quality of our own work, we improve the entire body of work in any scientific field.


## Editorial Board:

**Editor-in-Chief - Dr. Chuck Easttom** (Capitol Technology University, USA)
**Associate Editor - Dr. Nabeeh Kandalaft** (Grand Valley State University, USA)

**Board Members -**

**i) Dr. Phillip Bradford** (University of-Connecticut-Stamford, USA)
**ii) Dr. Alex "Sandy" Antunes** (Capitol Technology University, USA)
**iii) Dr. Izzat Alsmadi** (Texas A&M, San Antonio, USA)
**iv) Dr. Lo'ai Tawalbeh** (Texas A&M University-San Antonio, USA)
**v) Dr. Doina Bein** (California State University, Fullerton, USA)
**vi) Dr. Hasan Yasar** (Carnegie Mellon University, USA)
**vii) Dr. Moises Levy** (Florida Atlantic University, USA)
**viii) Dr. Christian Trefftz** (Grand Valley State University, USA)
**ix) Dr. Petros Spachos** (University of Guelph, Canada)

# APPLICATION OF THE "METHODOLOGY ASSESSMENT FRAMEWORK (MAF)" ON AN EDA TOOL DEVELOPMENT PROJECT

Ebru Dalbudak
*Computer Science and Engineering, Université du Québec en Outaouais*
Gatineau, QC, J8Y 3G5, Canada
dale02@uqo.ca

Karim Baratli
*Computer Science and Engineering, Université du Québec en Outaouais*
Gatineau, QC, J8Y 3G5, Canada
bark07@uqo.ca

Yousef Fouzar
*Computer Science and Engineering, Université du Québec en Outaouais*
Gatineau, QC, J8Y 3G5, Canada
yfouzar@yahoo.ca

Bachir Lakhssassi
*Computer Science and Engineering, Université du Québec en Outaouais*
Gatineau, QC, J8Y 3G5, Canada
Lakb01@uqo.ca

Karim El Guemhioui
*Computer Science and Engineering, Université du Québec en Outaouais*
Gatineau, QC, J8Y 3G5, Canada
Karim.elguemhioui@uqo.ca

Ahmed Lakhssassi
*Computer Science and Engineering, Université du Québec en Outaouais*
Gatineau, QC, J8Y 3G5, Canada
Ahmed.lakhssassi@uqo.ca

**Abstract—With the increased level of complexity and market pressures to deliver better results faster and cheaper, Integrated Circuit (IC) companies are looking to innovate and introduce efficiencies into their development process. To improve IC design productivity and time-to-market, this paper introduces an innovative Electronic Design Automation (EDA) tool in order to replicate an existing layout in different technology nodes by automatically porting analog and mixed-signal circuits. Furthermore, the paper presents a case study of the application of the Methodology Assessment Framework (MAF) as an evaluation tool to choose the best suited Software Development Methodology (SDM) for the EDA tool development project.**

**Keywords— IP Porting, IC design productivity, EDA, Technology Migration, Layout Migration, SDM, agile**

## I. INTRODUCTION

Integrated Circuit (IC) design complexity has been exponentially increasing since the appearance of transistors in 1958 [1]. Each generation of IC design process introduces improvements such as reducing the size of the transistors and wires and while increasing the number that can fit on a chip. Consequently, this allows the chips to run at higher frequencies and then the new designs get more sophisticated.

As the process technology advances, IC design rules[1] that are provided by semiconductor manufacturers to determine what can and cannot be manufactured also get more complicated and usually they are not compatible with previous generations [2]. According to Zhu et al.[3], "manufacturing processes are updated every 18 months each with a different set of design rules", and companies need to offer different versions for different foundries. The standard cell library, which consists of standardized layout specific components, for each process update also increases [4]. As a result, regenerating a new standard cell library for each process update gets more costly and time consuming [4, 5]. Moreover, the circuits need to migrated to work with the new target technology and this requires a tedious, often manual process of iterating layout changes, extraction and simulation until desired characteristics are met [1].

To maximize their design investments and reduce their design duration, Intellectual Property (IP) providers reuse blocks and hard IP whenever possible. At the beginning of or during a new IC design project, it is often necessary to use and re-use available IP and circuits from previous projects, instead of designing everything from scratch [6, 7]. Design reuse makes it faster and cheaper to design and the time lost by completely re-designing an existing circuit in another technology process can then be spent on new parts of the system that add extra functionality and/or increase performance and productivity [8].

Furthermore, since IC companies choose to outsource the fabrication of their semiconductor chips to foundries (by going fabless), they need to migrate their existing circuit designs "between process technologies and within internal and external foundry processes" because, frequently, foundries differ in their versions even if they use same process technology node [7]. Particularly, the number of metal layers, material table, etc.

Hence, there is a growing need in the semiconductor market to migrate an existing circuit layout between different technology

[1] Design rules determine whether the physical layout of a given circuit satisfies a series of recommended parameters to ensure that most of the parts will work correctly.

nodes and foundries in a reliable, fast and cost efficient manner [2, 3, 8, 9]. To produce designs quickly and to address design challenges, IC companies have been increasingly making use of the EDA tools [1].

This paper introduces two innovative approaches that will improve IC design productivity and hence will facilitate faster semiconductor development and time-to-market. First, it introduces a new EDA tool in microelectronics which aims to automatically port analog and mixed-signal circuits between technologies nodes in the hard IP market. Next, it presents the application of a new framework called Methodology Assessment Framework (MAF) on this EDA tool development project to demonstrate how the agile methodology was chosen to be the best suited SDM to promote the adaptive planning and evolutionary development and delivery of a module of this tool using short and iterative development cycles.

The article begins with introducing concepts relevant to the study as an overview. Next, it provides a detailed discussion on layout porting and its challenges. The paper continues with the introduction of the new EDA tool called OPIC that can help better manage the complexity in microelectronics for IP design porting of analog and mixed signal circuits between technology nodes. It proceeds with the case study on the use of agile methods during the development of a Design Rule Check (DRC) clean-up module of the OPIC tool. And it ends with concluding remarks.

## II. BACKGROUND / RELATED WORK

There are studies that were focused on IP reuse and technology migrations due to their expected benefits.

Sobe et al. [10] presents a method, that reflects common practice of analog design divided into design data conversion and sizing by optimization, to convert and optimize a circuit topology. Fu et al. [11] introduce a new rectangular topological layout for topology-driven cell migration. Kar et al. [12] talks about the technology migration process and introduce a new layout preserving migration tool called: TECHMIG. Francken et al. [6] presents a methodology for the migration of analog circuit design from one technology process to another, considering both the sizing and the layout phase. Diodato et al. [13] discuss porting of 2.5 micron CMOS VLSI design into 1.75 micron design rules. They were able to implement the new design in 33% less time and achieved smaller size in design rules by 19% and higher operating frequency by 43%. Dornelas, Helga et al. [5] introduced a new technology migration methodology for analog IC design and instead of doing the migration manually or at netlist level, they performed automated migration on a schematic level, followed by a robustness verification with the usage of MunEDA tools [5, 10].

However, literature review has revealed that even though there is abundant research in the field of IP reuse, design migration and layout porting, their use in analog and mixed-signal circuits is not as common [2].

The literature review on the EDA tools and the use of agile in IC development projects has proven that the use of agile methods in hardware development projects is not as common as in software development projects [14]. Innovation is a great challenge in the EDA industry and to provide faster, better, and cheaper products, the major players in the industry focus on improving existing tools and methodologies [15]. According to Bryant et al. "The quality of the design tools and associated methodologies determine the design time, performance, cost and correctness of the final system product" [16].

## III. LAYOUT PORTING

As Francken et al. stated "porting successful designs from one technology to another can distinctly reduce the design cycle" [6]. The aim of layout porting between technological process nodes is to be able replicate an existing layout (reference design) in different technology nodes by modifying or adapting it to a newer process design rules by taking advantage of the reusability of the layout resources accumulated from the initial process. Semiconductor foundries continue to innovate by continuous scaling of transistors. There is a growing need to redesign mixed signal circuits for new technological processes. The analog domain still lacks automation, which resulted in a manual design of analog circuits each time to migrate from one technology to another. While doing that the ultimate goal is to "achieve high quality layout with high integration and low power consumption and to shorten the design-time-to-market" [8]. This way, instead of spending time and effort from scratch to completely redesign an entire circuit, semiconductor companies can focus on innovation by adding new functionalities into their designs and focusing on increasing performance [6].

IC products are usually mixed signal designs, in other words, they comprise of a combination of digital and analog functional blocks and circuits and the analog portions of these ICs are the most difficult portions of the chip to migrate between foundries and technology nodes [2, 17, 18]. In digital designs, reuse of IPs has already been well established thanks to fully automated digital workflow [8]. However, in analog circuit designs, reuse of IP have challenges, such as "coping with trade-offs among analog specific requirements, such as noise, linearity, gain, supply voltage, speed, power consumption, self-heating, etc" [8].

Porting an existing design from technology A to technology B usually follows a two step design flow. In the first step, the given schematics and topologies are converted from the source to target technology and existing layout and mapping layers are migrated by recognizing different structure and device placements; preserving all floorplan, matching, routing and interconnect within the given layout [7, 19]. In the second step, these circuits and IPs are sized for the new target specifications and optimized for the new target process technology. Then, Design Rule Check (DRC) verification is conducted to preserve all matching within given layout and all routing and interconnect and Layout Versus Schematic (LVS) will be performed to ensure that the layout conforms to the rules required for faultless fabrication and performance [4].

At the present moment, in the IC design process, schematics and layout design phases are carried out sequentially. We start with the original reference design (for example 65nm), when the technology changes and we want for example 45nm technology node, we need to first migrate the specs (voltage is different, Vref(min, max)); get the schematics and circuit topologies for the new technology; translate schematics and topologies from 65nm process technology to 45nm process technology (via script); port the schematics from 65nm to 45nm; verify schematics; then use the schematics to generate/port the layout from 65nm to 45nm and verify the layout created in 45nm. As can be seen, in this type of a design, we do not take advantage of IP-reuse; design that works in one technology will not work in the other technology. So, IP has to be completely redesigned when the technology changes, which leads to more errors in the new design, added time, cost and human resources. Just to give an idea, today, about 100 engineers work together to design a new IP.

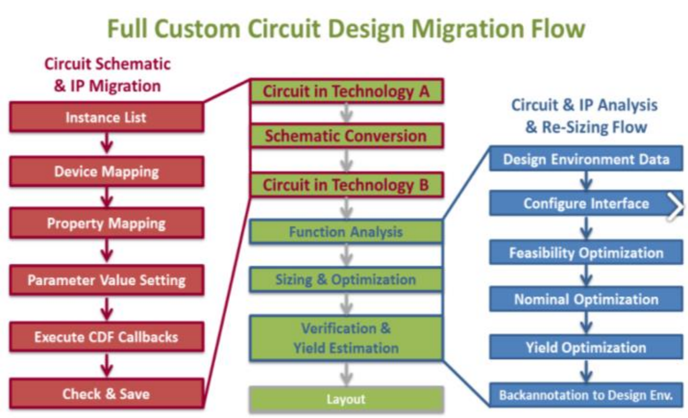


Figure 1: 2 steps of an IP Migration & Porting Flow [4]

## IV. New Layout Porting Tool: OPIC

This paper introduces a new automated layout porting tool to increase the effectiveness and efficiencies of the design conversion process by reducing the human resources required and by shortening the porting time while reducing the failures during conversion.

There are some target layout recognition and conversion tools available commercially. However, these tools perform porting only when the reference design and the target technology is highly specialized (e.g. microcontrollers, etc.) and homogeneous (e.g. FPGA to FPGA).

Available commercial tools do not include features like automatic porting between technology nodes and foundries for analog and mixed-signal circuits; they do not re-use the existing layout by making changes on it; instead they regenerate the layout from scratch using traditional manual porting methods. Given the size and complexity of each migration, traditional manual porting methods are too time-consuming and costly. They are also risky and human intervention could impact the quality of the IP resulting in the loss of work that was already done in previous technology. IC designers need to reduce a risk of having costly design bug during the manual porting process from scratch. Therefore, the new layout needs to be retested rigorously for reliability, which impacts the IP delivery timelines. Moreover, instead of losing their precious time on repetitive manual tasks, IC designers should rather focus on using their creativity and precision crafting their designs.

A tool that would automatically migrate any IP design and porting flow with minimum human intervention from one foundry specific technology to another would be invaluable for any IP provider. By using this kind of an automated tool, semiconductor companies can increase the efficiency of their IC design process by reducing the porting time and the risk of creating bugs or errors, as well as the costs.

OPIC, which stands for “Outil de Portabilite entre technologies des Circuits Integrés/ Porting Tool for Integrated Circuits”, is a new EDA tool that is designed for hard IP market to automatically perform the porting tasks with minimum human intervention and replicate an existing analog/mixed-signal circuit design (reference design) within different foundries and technology nodes.

The OPIC tool responds as well to an immediate need in the field of semiconductors and historical transition from traditional planar CMOS transistors to FinFETs, which is pending any adequate solution. The tool will be particularly useful in a variety of different important sectors, including IP providers, silicon foundries etc. within the semiconductor industry.

This automated porting tool is a type of back-end design tool, which aims to provide a quick and robust analysis of IP using existing layout, floorplan and routing between the blocks and will generate a DRC (Design Rule Check) and LVS (Layout Versus Schematic) clean layout in the targeted technology with minimum human intervention. The tool will port the graphical patterns (polygons) for each transistor and wire on the IC from one technology to another while preserving the key characteristics of an existing layout including matching of critical components and their relative placement in order to create a layout design that will function properly when fabricated.

The tool follows two major steps; first it will create a DRC and LVS database in technology B and then will perform circuit optimization and reflect schematic changes onto a clean layout.

The OPIC tool can be used to do the circuit and IP porting of a layout in source technology A to target technology B by converting the given schematics and topologies from the source to the target technology. It checks the geometries against geometry design rules, detects design rule violations according to specified IC parameters and automatically cleans them iteratively. As a final product, it generates an IC design in GDSII format, which is ready to be shipped to foundry for manufacturing.

The tool takes an existing design layout in a given technology (technology A), which consists of network of transistors and described by a geometrically exact Graphics Data System II (GDSII) file, which is the de facto industry standard for data exchange of IC design layout, and generates a new layout design in a different technology node (technology B) by using the design spec for the new layout in technology B and the technical mappings (for both A and B). which can be reviewed by a physical layout designer before it gets sent out to the foundry for manufacturing.


Figure 2: OPIC tool

To perform porting between two technological process nodes (from A to B), we need to have the following as input and follow the following steps listed below.

*Input:* Existing Layout Design in technology A in GDSII format, Design spec for the new layout in technology B, Technical mapping for technology A, Technical Mapping for technology B

*Steps:*
1. Open the given layout design in technology A with spec B and Existing Layout Design in technology A in GDSII format, Design spec for the new layout in technology B, Technical mapping for technology A, Technical Mapping for technology B migrate the layout into new layout design in technology B
2. Run the EDA tool called Design Rule Check (DRC) on Layout of technology B to identify the violations of design rules
3. Correct all the violations automatically and iteratively until the violations are cleaned
4. Obtain 100% accurate (target) layout for new design in technology B

*Output:* New layout design in technology B in GDSII format (binary file), which is ready to be given to IC foundries

We can run simulations on this new layout design in technology B to test it further and send this layout to a Physical layout designer for verification before the design gets sent to the foundry.

## V. Case Study: The Use Of methodology assessment framework (MAF) In the OPIC Project

### A. *The MAF framework*

Selecting the appropriate SDM for a project is one of the most important steps to ensure the project success [20, 21]. There are so many SDMs in the market but how do we choose the right one? How do we determine and measure the concept of “fit” between the chosen SDM and the project? According to Mullaly & Thomas, “attaining fit suggests that there is an alignment between what is being implemented and the environment and situation of an organization”[22].

The literature review has proven that there are several frameworks that have been used to define, compare and evaluate SDMs [23-26]. However, there is yet no comprehensive framework that uses the crucial factors to determine whether the traditional/plan-driven/waterfall, agile or hybrid type of system development methodology would be most suited for a project. Existing evaluation frameworks lack several aspects. Most of them have not considered evaluating agility. The nature and the complexity of the project as well as the extent and enrollment of the project’s constituent base have been neglected or only partially addressed. To address the need of a comprehensive evaluation framework, this paper has identified seven factors that are critical to providing the project’s executive sponsor and governance body with a dashboard view over the project landscape. They are as follows:

1. Outcomes being addressed by the project (OUTCOMES)
2. Scope /features of the project (SCOPE)
3. Nature and complexity of the project - CYNEFIN framework (CYNEFIN)
4. Extent and enrollment of the project’s constituent base (CONSTITUENTS)
5. Applicability of Agile principles to the project (AGILE PRINCIPLES)
6. Team expertise and experience in system development methodologies (TEAM)
7. Maturity of the organizations involved on the project (ORGANIZATION)

This paper introduces a new framework called “Methodology Assessment Framework (MAF)” as a tool that is based on these seven decision factors to come up with an overall assessment of a project to help determine the software development methodology approach that is best suited.

The OPIC project was evaluated against the seven factors of MAF (Outcomes, Scope, CYNEFIN, Constituents, Principles, Team, and Organization), using a series of self-evaluation tools that have been developed for each.

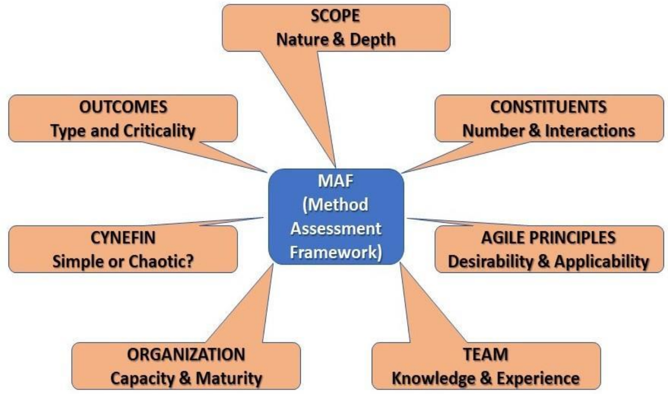


Figure 3: MAF framework and its 7 decision factors

The MAF suggested that an agile methodology is best suited SDM for this project because the project scored very low on Outcomes, Scope and Constituents dimensions while reasonably high on the CYNEFIN, Organization, Team and Agile Principles dimensions as demonstrated in the table below and using the radar chart in Figure 4.

| **MAF factors** | **Description** |
|---|---|
| **Outcomes** | Important - The number and criticality of outcomes have a bearing on the development method selected. |
| **Scope** | Small project with low complexity |
| **Constituents** | Small project, few constituents with basic role (*Inform*, *Consult* or *Educate)* |
| **CYNEFIN** | Complex, with a bit of uncertainty, innovation and experimentation are required, problems and solutions are evolving |
| **Organization** | Established in terms of organizational capacity and maturity |
| **Team** | Advanced, in terms of skills and expertise |
| **Principles** | 100% supports agile values and principles |

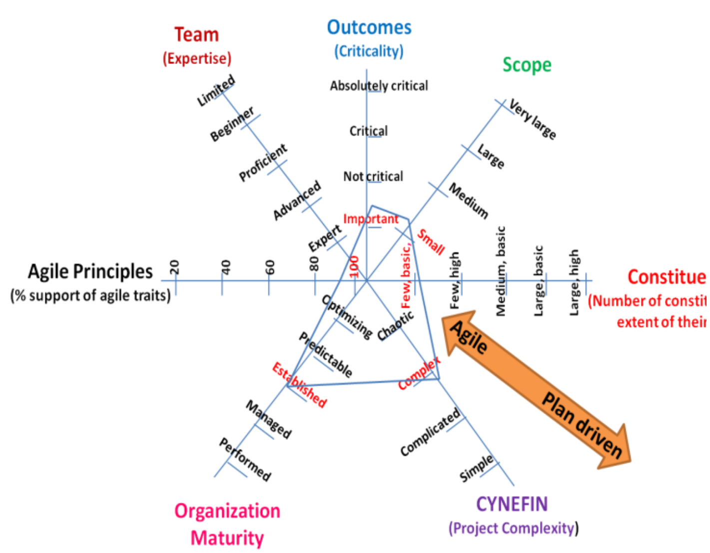


Figure 2: The MAF evaluation of the OPIC project using Radar Chart

## *B. The Use of Agile SDM in the OPIC Project*

OPIC tool is a long term project being developed in phases, module by module. DRC rule cleanup is the first module of OPIC that was implemented successfully tested. DRC checks if the layout satisfies a set of design rules required for manufacturing. If the design rules are violated, the chip may not be functional.

OPIC DRC cleanup tool was implemented using JAVA and it is compatible with major EDA tools, such as Cadence, Mentor Graphics and Synopsys. The tool has been tested to ensure that it can correct DRC errors on a given layout (in GDSII file format) and the results have shown that the tool could reduce the tedious work of DRC checking from 25 hours of manual porting labor to 30 sec as demonstrated in the table below.

| Reference Design | # and type of Errors | Manual correction | OPIC DRC Clean-up Tool |
|---|---|---|---|
| BIAS_GENERATOR | 56 (7 type violations: Overlap, spacing, width, extension, clearance, etc.) | 50 minutes | 30 seconds (24 CPU) |
| Oscillator (7x7 inverters, 0,18nm) | 378 (7 type violations: Overlap, spacing, width, extension, clearance, etc.) | 240 minutes (no MACRO used, assuming different errors and no compaction problem) | 183 seconds (24 CPU) |

65nm and 28nm technology nodes were the two platforms used for verification. A reference design including various analog and mixed-signal circuits was built in 65nm technology and OPIC DRC tool was used to determine if the layout satisfied a set of rules required for manufacturing to migrate it to 28nm.

OPIC DRC clean-up is based on a proprietary algorithm (similar to the backtracking/shrinkage algorithm) and it includes 10 categories of common DRC errors that are related to spacing between metals, minimum width, etc. These errors are PO.C.2 (Polysilicon Oxide layer, Clearance), M1.W.1 (Metal Layer – Width), NW.W.1 (N-Well Layer, Width), NW.W.2 (N-Well Layer, Width), NW.S.1 (N-Well Layer, Spacing), NW.S.2 (N-Well Layer, Spacing), M1.S.1 (Metal Layer, Spacing), CO.E.2 (Contact Enclosure), NP.E.1 (N-doped Poly/substrate, Enclosure), PO.O.1 (Polysilicon Oxide layer, Overlap). An engine for correcting each error category was created. The tool recognizes these 10 different DRC errors and based on the error category it selects the engine that will correct the error. Until all the errors are cleaned-up and the DRC is clean, the tool runs iteratively, without human intervention.

OPIC DRC tool was developed by using a combination of agile software development and agile project management methodologies. The project was evaluated against the seven dimensions of the MAF framework and agile methodology was identified as the best suited SDM. As a result, instead of defining the whole requirements, resources, technologies and tools upfront by using a plan-driven methodology like a waterfall, an agile development process was adopted, where the requirements, design and the process emerge in parallel during short, iterative cycles called *sprints*.

As shown in Figure 5 [27], the software development was based on an iterative life cycle and in one iteration cycle, an increment of the software was analyzed, designed, built, tested and integrated on a continuous basis until the full solution was realized [28]. At the end of each iteration, a subset of functionality was delivered to stakeholders for review and the software was built incrementally, piece by piece [29]. This way, the overall risk was minimized and the project could adapt to changes quickly.

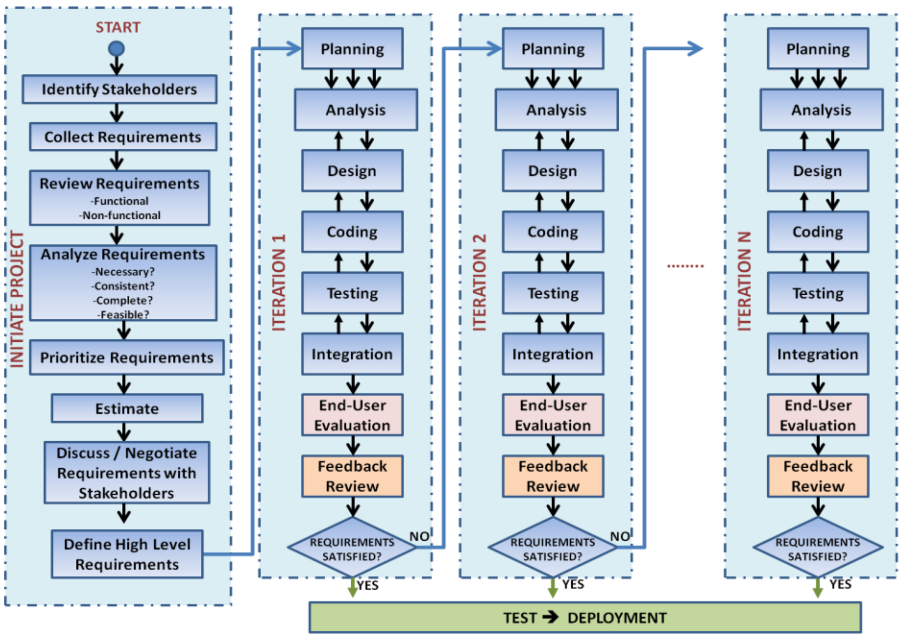


Figure 5: Agile Development methodology used in the OPIC project

To be more specific, a hybrid agile approach of eXtreme Programming (XP) and SCRUM (where XP engineering practices are implemented in SCRUM sprints) were chosen and adopted in this project. According to Agile Alliance[2], "XP is an agile software development framework that aims to produce higher quality software, and higher quality of life for the development team" while SCRUM is a project management approach.

XP focuses on the developer side of the work with a set of engineering practices it mandates such as test driven development, pair programming, continuous integration, etc. which are very essential for building good quality software. SCRUM focuses on the project management side on what needs to be done. Since SCRUM does not have any engineering practices and XP does not have any management practices, XP and Scrum are well aligned and complement each other.

In the OPIC DRC tool project, the best practices recommended by XP were used for agile software development, such as simple design, pair programming, and small, frequent releases. SCRUM project management framework was used to manage the steps taken to develop software in conjunction with the use of XP to ensure the quality of the software.

This project was led by a project manager, who was responsible for coordinating the work of the cross-functional, self-organizing Scrum team of 5 people and for ensuring that tasks were completed within the scheduled time. The work was broken down to fit 3-week long sprints. Each sprint includes the traditional phases of software development: requirements analysis, design, coding, testing.

As shown in Figure 6, at the beginning of each sprint, a Sprint Planning meeting was held to plan the work to be done during the given sprint. In this meeting, a Sprint backlog that contains all the user stories (work items) to be implemented during the sprint was created, reviewed and prioritized. The team had daily scrum meetings of maximum 15 minutes to review the progress and productivity, to synchronize the information and to address the blocking issues. Team members worked on the user stories until completed. At the end of each sprint, a Sprint review meeting was held to demonstrate the work that was completed during the sprint and to gather feedback. The Sprint retrospective meeting was held shortly after that to reflect upon the last sprint in order to identify what went well and possibilities for improvement.

[2]A non-profit organization dedicated to promoting agile methodologies at agiilealliance.org

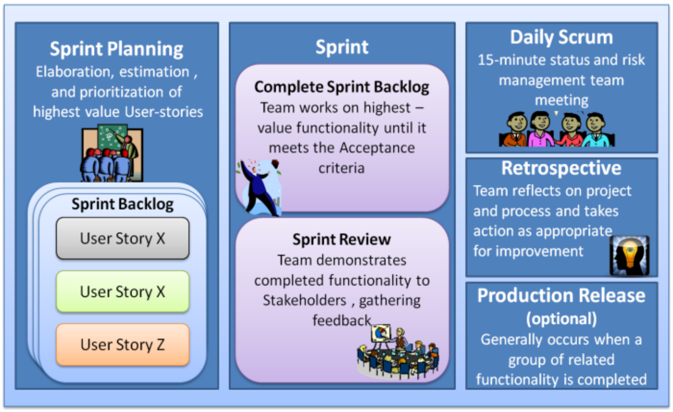


Figure 6: Scrum model that was followed in the OPIC project

Agile methodology was successfully adopted in this project to deliver the OPIC DRC tool in an iterative, incremental approach. Combining two agile approaches XP (for development practices) with Scrum (for project management) proved to be effective. Planning and big-picture view was crucial. Everyone in the team needed to understand what they were working towards for each piece to be able to come together in the end. Establishing an upfront, common understanding of the criteria for done-ness for each user story, for each sprint and for the release was very necessary. Clear and open communication was paramount. Note that agile mindset had to be understood and embraced by everyone in the team it took some time to refine the Scrum model to the point where team members were comfortable and productive.

## VI. Conclusion

Due to the complexity of recent advanced technology nodes, no automatic or pseudo-automatic tool has been developed for IP porting yet. This paper has introduced a new EDA tool called OPIC that will automate porting of analog and mixed signal circuits from one technology node to another.

To select the appropriate SDM in order to maximize the chance of project success, the paper also introduced a new framework called MAF and used this framework to assess and evaluate an IC development project by using the OPIC DRC tool project as a case study. As per the MAF framework evaluation, which identified agile methodology as the best suited SDM for the project, the paper also presented a real-life example of adopting a hybrid agile methodology (combination of XP and SCRUM) in the OPIC DRC tool project.

Automated OPIC DRC cleanup tool represents a major step for layout porting. This tool could be used as a standalone product and integrated with major commercially available tools to perform a DRC cleanup. It will allow designers save a considerable amount of time and use this time to focus on precision crafting their designs without sacrificing creativity to repetitive manual tasks.

Once fully implemented, OPIC tool will perform both the DRC and LVS corrections, automatically. So, the next step is to create an LVS tool, which takes a schematic to identify and check IC electrical connectivity against IC schematics and makes corresponding changes on the layout.

The need for increased capacity for more complex chips, speedups and new capabilities is growing and the time-to-market is getting shorter, increasing design productivity by utilizing IP-reuse and EDA tools will continue to play a critical role in semiconductor design and development.

As for the MAF framework, further empirical research is recommended to refine and update the proposed framework and apply it to assess various projects of different size and complexity.

## References


1. Birnbaum, M.D., *Essential Electronic Design Automation (EDA).* Prentice Hall PTR/Pearson Education, 2004.
2. Scheible, J. and J. Lienig. *Automation of analog IC layout: challenges and solutions*. in *Proceedings of the 2015 Symposium on International Symposium on Physical Design*. 2015. ACM.
3. Zhu, J., F. Fang, and Q. Tang, *Calligrapher: a new layout-migration engine for hard intellectual property libraries.* IEEE Transactions on Computer-Aided Design of Integrated Circuits and Systems, 2005. **24**(9): p. 1347-1361.
4. ME, M.N.R.K., *DEVELOPMENT OF HIGH PERFORMANCE STANDARD CELL LIBRARY IN UMC180nm TECHNOLOGY.* International Journal of Advanced Research in Electronics and Communication Engineering (IJARECE), 2014. **3**(9).
5. Dornelas, H., A. Schmidt, G. Strube, and E. Fabris, *New Technology Migration Methodology for Analog IC Design.*
6. Francken, K. and G. Gielen. *Methodology for analog technology porting including performance tuning*. in *Circuits and Systems, 1999. ISCAS'99. Proceedings of the 1999 IEEE International Symposium on*. 1999. IEEE.
7. MunEDA *Automated Design Migration & IP Porting Flow for Custom Circuits*. 2014. https://www.muneda.com/Applications_Custom-Circuit-Design-Migration-&-IP-Porting.
8. Nojima, T., S. Nakatake, T. Fujimura, K. Okazaki, Y. Kajitani, and N. Ono. *Adaptive porting of analog IPs with reusable conservative properties*. in *IEEE Computer Society Annual Symposium on Emerging VLSI Technologies and Architectures (ISVLSI'06)*. 2006. IEEE.
9. Qian, L., Z. Bi, D. Zhou, and X. Zeng, *Automated technology migration methodology for mixed-signal circuit based on multistart optimization framework.* IEEE Transactions on Very Large Scale Integration (VLSI) Systems, 2015. **23**(11): p. 2595-2605.
10. Sobe, U., A. Graupner, E. Böhme, A. Ripp, and M. Pronath. *Analog ip porting by topology conversion and optimization*. in *IP-ESC09 Conference*. 2009.
11. Fu, D.-S., Y.-Z. Chaung, Y.-H. Lin, and Y.-L. Li. *Topology-driven cell layout migration with collinear constraints*. in *Computer Design, 2009. ICCD 2009. IEEE International Conference on*. 2009. IEEE.
12. Kar, P.K. and S.K. Roy. *TECHMIG: A layout tool for technology migration*. in *VLSI Design, 1999. Proceedings. Twelfth International Conference On*. 1999. IEEE.
13. Diodato, P., A. Goksel, F. La Rocca, and W. Troutman. *Porting of a CMOS VLSI Chip from 2.5 Micron to 1.75 Micron Design Rules*. in *Solid-State Circuits Conference, 1984. ESSCIRC'84. Tenth European*. 1984. IEEE.
14. Johnson, N. *Agile hardware development–nonsense or necessity*. EE Times, 2013. https://www.eetimes.com/agile-hardware-development-nonsense-or-necessity/#.
15. Sangiovanni-Vincentelli, A., *The tides of EDA.* IEEE Design & Test of Computers, 2003. **20**(6): p. 59-75.

16. Bryant, R.E., K.-T. Cheng, A.B. Kahng, K. Keutzer, W. Maly, R. Newton, L. Pileggi, J.M. Rabaey, and A. Sangiovanni-Vincentelli, *Limitations and challenges of computer-aided design technology for CMOS VLSI.* Proceedings of the IEEE, 2001. **89**(3): p. 341-365.
17. López, R.C., F.V. Fernández, Ó. Guerra-Vinuesa, and Á. Rodríguez-Vázquez, *Reuse-based methodologies and tools in the design of analog and mixed-signal integrated circuits*2007: Springer Science & Business Media.
18. Macintosh, M., *Analog Hard IP made portable.* Chip Design Magazine, 2014.
19. Payne, D. *Three Steps for Custom IC Design Migration and Optimization*. 2016. https://www.semiwiki.com/forum/content/6140-three-steps-custom-ic-design-migration-optimization.html.
20. Chow, T. and D.-B. Cao, *A survey study of critical success factors in agile software projects.* Journal of Systems and Software, 2008. **81**(6): p. 961-971.
21. Misra, S.C., V. Kumar, and U. Kumar, *Identifying some important success factors in adopting agile software development practices.* Journal of Systems and Software, 2009. **82**(11): p. 1869-1890.
22. Mullaly, M. and J.L. Thomas, *Exploring the dynamics of value and fit: Insights from project management.* Project Management Journal, 2009. **40**(1): p. 124-135.
23. Micic, L. *Agile methodology selection criteria: IT start-up case study*. in *IOP Conference Series: Materials Science and Engineering*. 2017. IOP Publishing.
24. Taromirad, M. and R. Ramsin. *Cefam: Comprehensive evaluation framework for agile methodologies*. in *Software Engineering Workshop, 2008. SEW'08. 32nd Annual IEEE*. 2008. IEEE.
25. Griffiths, M., *Agile suitability filters.* Retrieved January, 2013.
26. Alqudah, M.K. and R. Razali, *Key factors for selecting an Agile method: A systematic literature review.* International Journal on Advanced Science, Engineering and Information Technology, 2017. **7**(2): p. 526-537.
27. Dalbudak, E., El Guemhioui Karim, Lakhssassi Ahmed, *On the Use of Agile Methods for IC Design*, in *28th International Conference on Computer Applications in Industry and Engineering (CAINE 2015)*2015: San Diego, California.
28. Highsmith, J., A. *What is Agile Software Development?* CROSSTALK The Journal of Defense Software Engineering, 2002. http://www.adaptivesd.com/articles/cross_oct02.pdf.
29. Fowler, M. and J. Highsmith, *The agile manifesto.* Software Development, 2001. **9**(8): p. 28-35.

# A New Approach Model of e-Visual Career Application in Distance Education

Mustafa TUNAY
*Department of Computer Engineering*
*Istanbul Gelisim University*
Istanbul, TURKEY
mtunay@gelisim.edu.tr

***Abstract*—A new approach for ranking visual career counselling based on distance measures is explained. In this paper, the traditional method of career counselling will be carried out by means of distance consulting services to make career counselling. Especially, professional education in the capacity limitation and professional working demand for education has led to a proliferation of virtual applications. Hence, e-Visual Career Application has been developed as a web-based program for clients who have taken professional counseling efficiently. With this application, it will help clients in the process of discovering and making decisions to their interests, abilities, personalities, skills and values. This paper relies on the implications of introducing online visual career consulting in the login sessions and how it affects the people (supervisor and client), the processes (consulting), and the organizations involved.**

***Keywords—Visual Career Counselling, Traditional Method, Virtual Application, e - Visual Career Application***

## I. Introduction

This career application system is done with specially developed software for providing more fruitful advising system on career development by considering interests, capacities, personalities, abilities and values that are developed in order to help people while they are discovering the right track and making decisions on their career development in this paper.

Distance education [1-2] is not a new concept and "Distance education", which eliminates the obligation of the instructor and the student to be in the same place; it is an education system, it is an alternative system to today's formal education system and its success rate increases day by day with the developing technology. Although a definite starting date cannot be determined but the use of distance education applications in an organizational structure is encountered in the 19th century.

In recent years, information and educational technology in distance education [3-5] have developed, while more information has been produced than in the past. These developments in distance educatrion changed the lifestyles of people, their needs and thoughts in obtaining information. As a result of the changes that occur in parallel with the development of educational technology in distance education, the most educational institutions is affected from globalization. Technological tools [6-7], which are always with individuals, increase the importance of the use of e-learning tools [7-10] for institutions and individuals to have an effective and productive structure in their career development. Thus, developing educational technology, reaching the information from the reliable sources and stating the references of the sources correctly can be considered as an important element in the development of societies [11]. For this reason, internet and computer are the most of the important communication tools which help people in reaching the scientific information on the right time.

The online education [12-14] system is a very important education system in order to prevent formal education that cannot be processed fluently, especially as a result of the measures taken against global problems. Thanks to online education, students can continue their education without delaying their courses for lost opportunity in face-to-face learning [15-17] and time and can repeat the topics covered on the system. In this regard, online education are conducted in 2 ways; asynchronous and synchronous [18-19]. Although distance education is called asynchronous education, but universities have unique learning management system (LMS) that can reflect their own characteristics and meet the requirements of the distance education applications [20] in today's world, adapt rapidly to technological innovations will arise in the medium and will provides synchronous education opportunities integrated into this system for a long term. Thus, this system as educational programmings [21-22] provide an interactive communication between instructors and students. Thanks to such educational programmings, it will be a important tools [23-24] that help students especially their career development skills.

Discovering the existence of new science, gaining new facts, and using that information in the right place and on the right time lead to new job areas (career development skills) for people in the world. It can be seen that most of the people from different profession needs to update themselves and their knowledge each passing day. Providing counselling services to the people who are in the working life actively will help them to address the need of the people around us and this will raise their activities in their profession. However in recent days, it can be seen that lack of counselling advisors cause the problems in the processing of the duties. For this reason, applying the use of “distance web-based advising career application” has a huge importance. This application is dealing with management of synchronous, asynchrony [19] and the mix of them when supervisor and client conducting the consulting service at the same time (synchronous), when the advisor and client learn and use the counselling material separately (asynchrony) and hence the application system as learning management system [25-29] that use both of them together is called as mixing. e-Visual Career Application (e-

Copyright © AJSE Publishers

VCA) System is a kind of distance web based for handling most of the career consulting activities as it can be done with face-to-face education. It is possible to have audio-visual communication with thorough independent career development advising career application system is also look like a face- to-face environment. Client may follow the notes of the counselling weekly, personal information forms, tests, measurements, inventory, technics and weekly research activities through this career application system, they may interact with their supervisors and they may communicate in login sessions. The scope of this career application system is to gather requirements, analyze, design, and develop the e-Visual Career Application website. The objective of this engagement creates e-Visual Career Application (e- VCA) for supervisors and clients that will achieve the following goal:

- Supervisors will be able to do the registration of the career application system on the internet.
- Clients will be able to attend lively meeting arranged before.
- A client registered in the system application will be able to access the counseling materials easily from their portal through this career application system.
- All the questions are raised by the client will be able to produce chain of discussion have a change to discuss with his/her supervisor through the career application system.
- Clients will get chance to ask for an extra meeting from their supervisors.
- This career application system consists 5 sessions and each session is 45-50 minutes in a week.
- Client will be able to do the personal information form, tests, measurements, inventories, techniques and weekly searching tasks on the career application system.
- The attendance of clients will be able to be followed by the advisors with the help of career application system. The supervisor will be able to arrange an extra meeting hourly and will be able to send the counseling materials on the web.
- This application system will be the center of most of the developmental areas related to teaching and learning with the raising application areas, with the harmony of the learning strategy, without any problem related to place and timeframe and with the flexible learning methods.
- With the scope of the career application system, the content of the counseling is prepared for five week and all the counseling materials will be open for supervisor during the year.

*1.1 Executive Summary*

Implementing the system application is using common internet technologies with PHP and Mysql as the backbone, provides staff with a tool to easily communicate, distribute information and facilitates collaboration across the entire organization.

*1.1.1 Technologies Used*

This career application system is a kind of web application and is developed as;

1. Database Design (MySql)
2. Coding (PHP)

*1.1.2 Browser Compatibility Statement*

We request you to use the career application system in the latest version of browsers and are available from the market. Because the older versions may not support and some design part of the career application system needs manual update or automatic update to keep up to date of web browser.

*1.1.3 Software Interface*

The purpose of this section is to define all online screens that are part of the career application system and their interdependencies and to provide details on the functionality of the screen based on a user's actions.

1. Web Server: .NET Framework, Web Browser.
2. Database Server : MySQL

*1.1.4 Security of System*

PHP (coding) is a fast and easy-to-learn language, for this reason, we can cause software-related security vulnerabilities. The proposed system data is protected with password-based logins by SSH key, or secure shell that is an encrypted protocol used to administer and communicate with servers. SSH Key is any kind of authentication, including password authentication and it is completely encrypted. Thus, SSH keys use encryption to provide a secure way of logging into your server and are recommended for all users. For SSH key authentication is showed in Figure 1. There is a important point for user must place your public SSH key on the server in its proper directory.

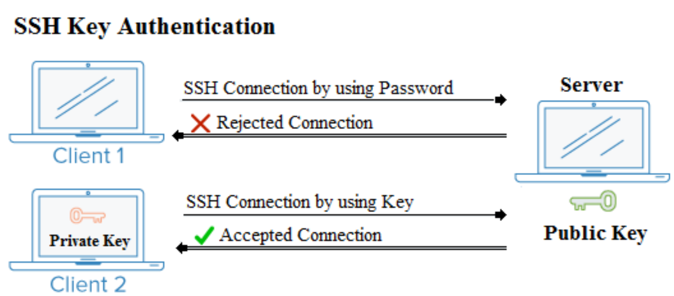


Fig. 1: Security of System by using SSH Key

According to SSH keys Authentication; a private and public key pair are created for the purpose of authentication. When password-based logins are allowed, malicious users can repeatedly attempt to access a server, especially if it has a public-facing IP address.

## II. THE APPLICATION SYSTEM

In a distance education process, there are many Learning Management System (LMS) applications provide learning content presentation in a web based learning as web server software (MySQL, Apache, Oracle e.g.) for performing learning content that can be used in many different phases as career application systems. The significant time required to develop scales has also been a consistent finding in studies involving distance education in career and technical education career application system. For this reason, e -Visual Career Application (e-VCA) *System* is a kind of distance web based for handling most of the career consulting activities. In Figure 2 shows that the details regarding the e-Visual Career Application (e-VCA), scales (files) and web server software are used in a career application system.

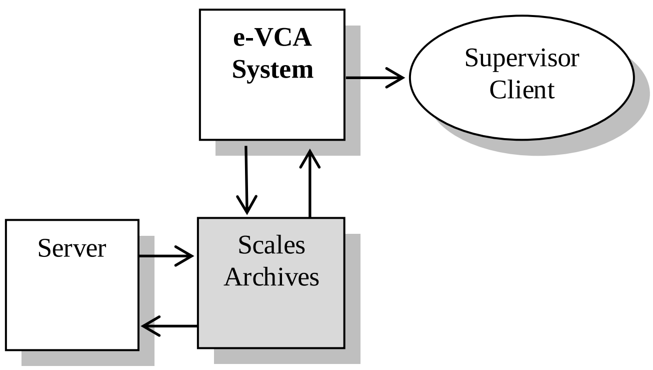


Fig. 2: e-Visual Career Application (e-VCA) and Web Server Software

The career application system is designed and represented the general scope with a contextual boundary of e-VCA System. It describes the main objective of the system and its entities involved functionality. This career application system is designed totally five steps to show how it is easy to start using its organization functionality such as; Login, the page of Home, Archives and Scales, Clients' Information and Sessions.

### *2.1 Login*

The first stage function is designed the page of login that is expected to play an important role in the conducting of online career counseling. The purpose of the login page is first required to register by from clients on the online website. This page also has access of the system that is secured by the login/password mechanism (by using private e-mail address) for the login id is created an account from the clients at the time of registration and provided it from their supervisors. Figure 3 shows that the details regarding the page of login in a career application system.

### *2.2 The Page of Home*

The second stage function is designed about view of registration information. The purpose of the home page has demonstrated views of total approved and unapproved clients are available. It has included how many total/active topics as personal information form, tests, scales, inventories, and research techniques weekly that are presented. In Figure 4 shows that the details regarding the page of home in career application system.

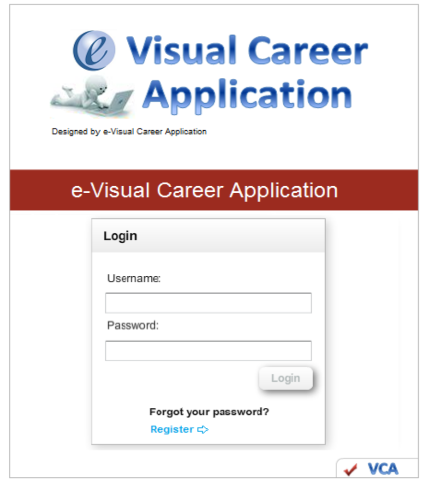


Fig. 3: The page of Login

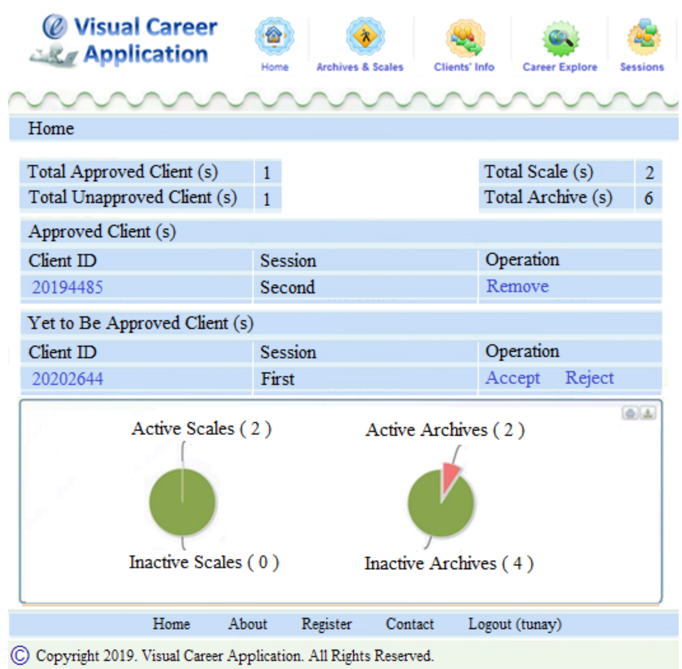


Fig. 4: The page of Home

Next one is about the lists of approved clients; it has been viewed with their information and supervisors can manage the client's information such as their control by hitting of remove link, the listing their information that are showed. Secondly, this part has two important roles as print option; it is about print out of summary for active and inactive documents. And next one is about chart; it also has option to download and view in various formats about clients' information. The detail regarding the page of Home is given in Figure 4.

*2.3 Archives and Scales*

The third one is designed the page of Achives and Scales; it has all privileges to edit/delete all the files /directories created by supervisor who uploads topics (personal information form, tests, scales, inventories, and research techniques) and clients can view all the files uploaded by supervisor according to their sessions. The detail regarding the page of Archives and Scales is given in Figure 5. Supervisor can manage all of information as sending new tests, scales, inventories and new sources for special member clients. They also can search any member of client and take information about searched the member client.

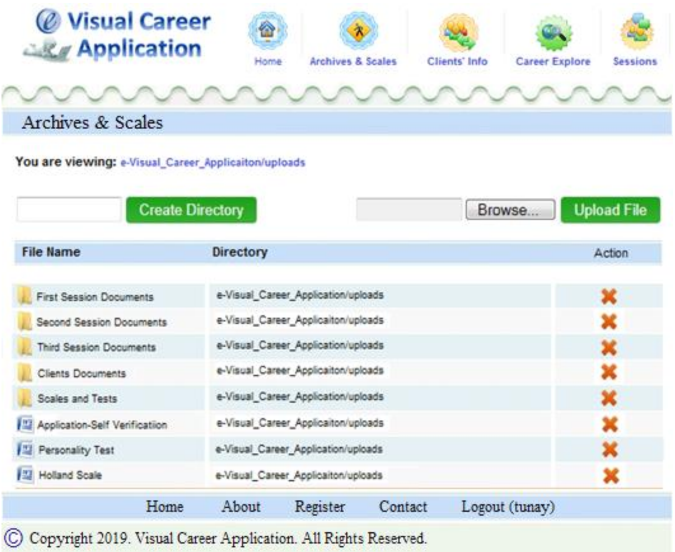


Fig. 5: The page of Archives and Sclaes

*2.4 Client's Information*

The fourth stage is designed for the page of Client info; it allows view of clients' situation (personality information, address, attending session and other information). It has two important roles as adding clients and editing clients.

*2.4.1 Adding Clients*

To add a client, go to the clients tab and fill in the form and click the add client button at the bottom of the page. Newly-added clients are automatically given active status, allowing them to sign-in to e-Visual Career Application immediately. However, newly-added clients must be told how to access e-Visual Career Application System that sent info feature to approved e- mail by using the activation with client information as username, password, and URL to sign-in.

*2.4.2 Editing Clients*

To edit a single client, click on his/her row, update their information, and click on the save changes button at the bottom of the page. To edit alter multiple clients at once by clicking on the checkbox next to their name (or select all by clicking on the checkbox in the header) in combination with the button at the bottom of the page.

Moreover, it gives change to supervisor can manage to keep certain clients from signing- in to e-Visual Career Application sets their account status as active or inactive. The detail regarding the page of Search is given in Figure 6.

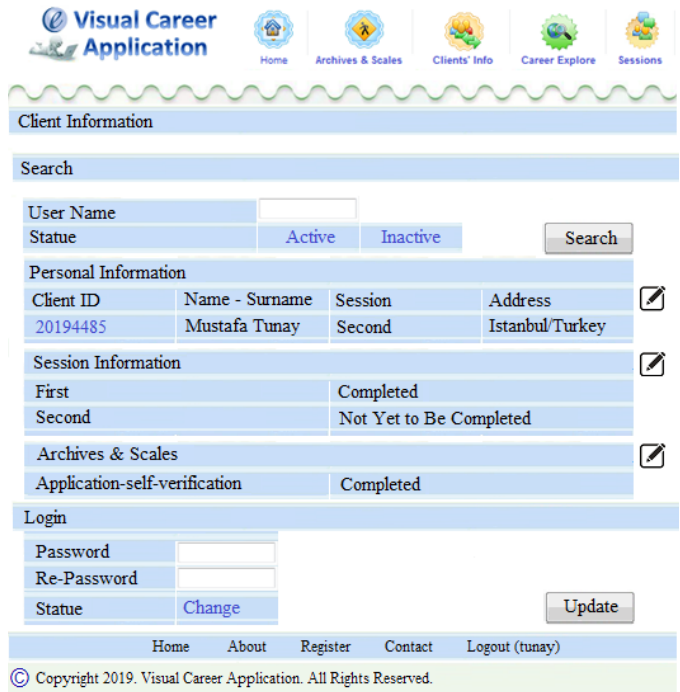


Fig. 6: The page of Search

*2.5 Session*

The last one is designed for the page of Session. Career Counselling consult with scales determined by the consultant to implement the system for the distance career education of the necessary personal information, forums, testing, inventory, and make appointment online interviews with five sessions and each session is determined as 45-50 minutes. In this context, e-Visual Career Application system offers online consultations that are relevant to the topic, inventory, scales (Holland or MBS), activities and the session on the techniques during last for five weeks. These sessions are as follows;

1. Session: Configuration and discovery.

2. Session: Scale and tests, and provide information about the application.

3. Session: Transmission of test results, and review of the advisory tasks.

4. Session: Duties discussion, brainstorming, information, research, and deal with the action plan.

5. Session: progress review, and if necessary to determine new goals.

At the same time, the client requests extra appointments to take any time from their supervisor by means of e-Visual Career Application system, session on the topic which is applicable to the person receiving vocational career education, carried out sharing inventories with supervisor electronically.

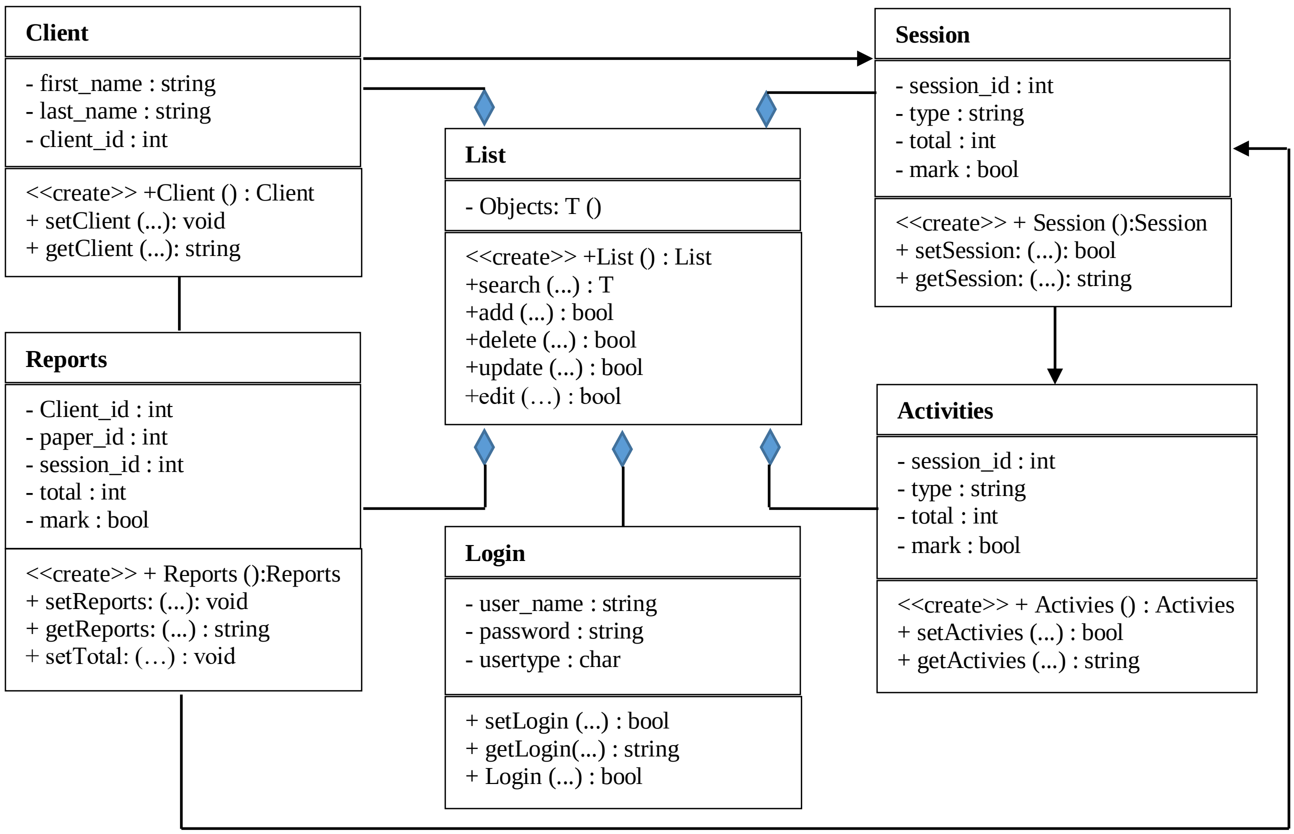


Fig. 10: The diagram model of the proposed system

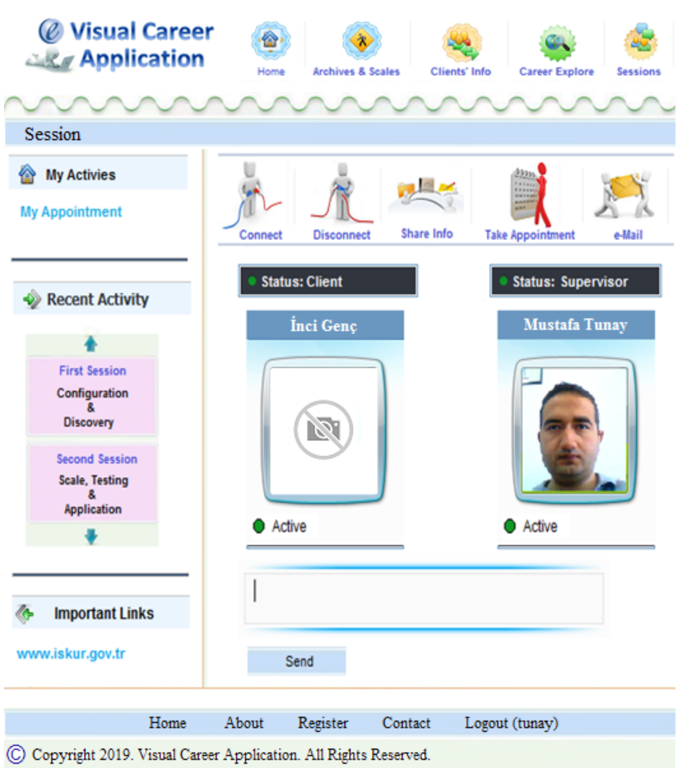


Fig. 7: The page of Session

This application system is applied on a blind student's İnci GENÇ at Eastern Mediterranean University in TRNC. She got the necessary personal information, forums, testing; inventory on the application system by using record voice, and make appointment online interviews with five sessions and each session was as 45-50 minutes with his supervisor. She got a great achievement at the end of five sessions. The detail regarding the page of Session is given in Figure 7.

This application system is ready to apply on close to graduate students (this semester) at Istanbul Gelisim University in Turkey for improving their career skills.

## III. The Model Application System

The model of career application system is designed with supervisor, client and functional activities are described. In Figure 8 represents what are the bounders and scope of e-Visual Career Application system. It describes the main objective of the system and is entities involved. Moreover, the diagram represents the general scope with a contextual boundary of e-Visual Career Application (e-VCA) system describes the main objective of the system and its entities involved. All details regarding the context diagram of proposed system is given in Figure 9.

This career application system is done with specially developed software for providing more fruitful advising system on career development by considering interests, capacities, personalities, abilities and values that are developed in order to help people for improving career skills in their future life and is figured out the overall system with its entities.

The model of e-Visual Career Application used sequence diagram generally and figure out the overall system. This model of diagram are interactions between a system's clients-system and supervisor-system with among objects in the system when relations occur with whole application system in Figure 10.

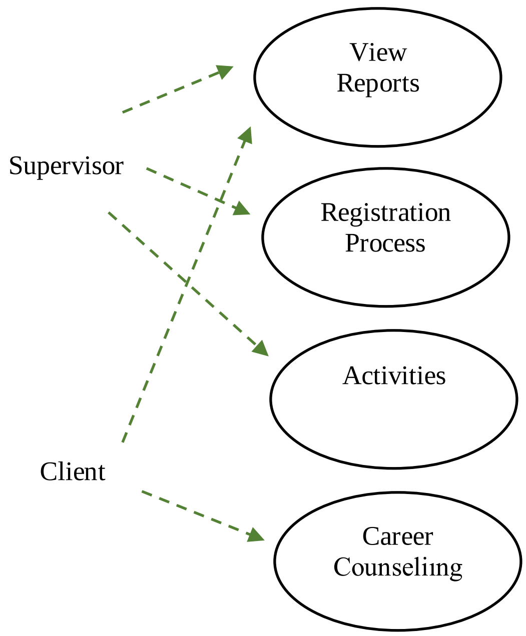


Fig. 8: The Model of e-Visual Career Application (e-VCA) System

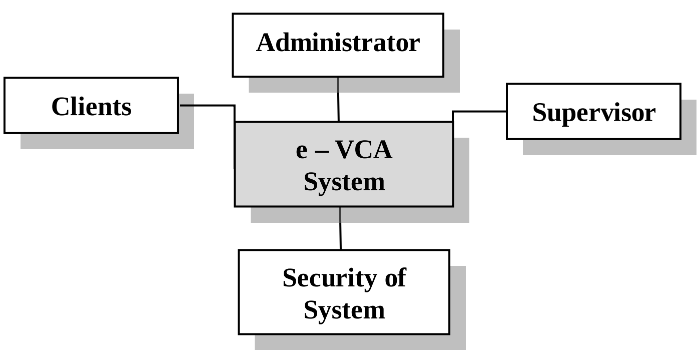


Fig. 9: The context diagram of e-Visual Career Application System

## IV. CONCLUSION

This paper proposes the e-visual career application system is designed for clients in helping to take professional career counseling efficiently and will help clients in the process of discovering and making decisions to their interests, abilities, personalities, skills and values. The designed career application system is included many features that improves pedagogical scales, inventory and many needed tools for of the academic disciplines, developing career in distance education programs utilize technology to a high degree. In addition, we can say that it is a system which is very useful and using time period for the specialists in terms of their distance, for the use of disabled people and new graduated students to improve their career skills in future life.

In the future, this study will need to be conducted to determine the most effective ways to utilize distance education in the delivery of professional career counselling.

## ACKNOWLEDGMENT

The author would like to thank Faculty of Engineering and Architecture, Department of Computer Engineering, Istanbul Gelisim University, Turkey.

## REFERENCES

[1] Distance Learning Resource Network. What is distance education? Retrieved April 23, 2003 from www.dlrn.org/library/dl/whatis.html.

[2] Oliveira, W. and Do Amaral, L. A. M. (2019). "Distance Education as a Service System," 2019 IEEE World Conference on Engineering Education (EDUNINE), Lima, Peru, 2019, pp. 1-6, doi: 10.1109/EDUNINE.2019.8875822.

[3] Flowers, J., (2001). Online learning needs in technology education. Journal of Technology Education, 13 (1), 17-30.

[4] Hillesheim, G. (1998). Distance learning: Barriers and strategies for students and faculty. Internet and Higher Education 1 (1), 31-44.

[5] Kanakana-Katumba, M. G. and Maladzhi, R. (2019). "Online Learning Approaches for Science, Engineering and Technology in Distance Education," 2019 IEEE International Conference on Industrial Engineering and Engineering Management (IEEM), Macao, Macao, 2019, pp. 930-934, doi: 10.1109/IEEM44572.2019.8978892.

[6] Tesone,D. V., Kelsey,R. L., Gibson, J. W. and Blackwell, C. W. (2002). "Using multimedia tools to enhance communication in the online classroom," *Proceedings. IEEE International Professional Communication Conference*, Portland, OR, USA, 2002, pp. 199-206, doi: 10.1109/IPCC.2002.1049103.

[7] Eroglu, M. A. (2009). "Academic document sharing at IAU members and distance education tools (samples of Turkish language)," *2009 International Conference on Application of Information and Communication Technologies*, Baku, 2009, pp. 1-5, doi: 10.1109/ICAICT.2009.5372589.

[8] Paulsen, M. F.; Keegan, D.; Dias, A.; Dias, P.; Pimenta, P.; Fritsch, H.; Föllmer, H.; Micincova, M. & Olsen, G., 2002. Web-Education Systems in Europe, Hagen: Zentrales Institut für Fernstudienforschung, Fern Universität.

[9] Vargas, R. P., Hortelano,M. R., Abad, L. T., Carrillo J. C., and Berlinches, R. H. (2018). "Teaching cloud computing using Web of Things devices," *2018 IEEE Global Engineering Education Conference (*EDUCON), Tenerife, 2018, pp. 1738-1745, doi: 10.1109/EDUCON.2018.8363444.

[10] Angles,R., Silvestre, L. and Pincheira, G. (2019). "Edutrivias: Web support system based on trivia for the teaching-learning process," *2019 38th International Conference of the Chilean Computer Science Society (SCCC)*, Concepcion, Chile, 2019, pp. 1-8, doi: 10.1109/SCCC49216.2019.8966392.

[11] Paloff, R., & Pratt, K. (1999). Building Learning Communities in Cyberspace. San Francisco: Jossey-Bass.

[12] Kanakana-Katumba, M. G. and Maladzhi, R. (2019). "Online Learning Approaches for Science, Engineering and Technology in Distance Education," *2019 IEEE International Conference on Industrial Engineering and Engineering Management (IEEM)*, Macao, 2019, pp. 930-934, doi: 10.1109/IEEM44572.2019.8978892.

[13] Shadmanova, G., Mirzaev S. and Karimova, X. (2019). "Upgrading Higher Education through Open Online Courses," *2019 International Conference on Information Science and Communications Technologies (ICISCT)*, Tashkent, Uzbekistan, 2019, pp. 1-3, doi: 10.1109/ICISCT47635.2019.9012019.

[14] Zhu, J. (2010). "A hybrid online-education strategy for delivering engineering and technology courses," *2010 International Conference on Networking and Digital Society*, Wenzhou, 2010, pp. 448-451, doi: 10.1109/ICNDS.2010.5479464.

[15] Swan, M., & Jackman, D. (2000). Comparing the success of students enrolled in distance education courses vs. face-to-face classrooms. Journal of Technology Studies, 24 (1). Retrieved March 11, 2003 from http://scholar.lib.vt.edu/ejournals/JTS/Winter-Spring-2000/swan.html.

[16] Merenkov, D. V., Shirinskii, S. V., Korkin, V. S., Zhokhova, M. P., Osipkin, S. V. and Dergachev, P. A. (2020). "E-Learning Resource for Electric Machine Design," 2020 V International Conference on Information Technologies in Engineering Education ( Inforino ), Moscow, Russia, 2020, pp. 1-4, doi: 10.1109/Inforino48376.2020.9111745.

[17] Talib, A. M. and Alomary, F. O. (2018). "An Interactive Distance Education and E-Learning System Based on Multi Agent System Architecture," 2018 1st International Conference on Computer Applications & Information Security (ICCAIS), Riyadh, 2018, pp. 1-6, doi: 10.1109/CAIS.2018.8441984.

[18] Miller, W.W., & Webster, J. K. (1997). A comparison of interaction needs and performance of distance learners in synchronous and asynchronous classes. Paper presented at the American Vocational Association Convention, Las Vegas, NV . (ERIC Document Reproduction No. 415 411).

[19] Timofeev, A. V., Tokarev, N. V. and Petrova, K. A. (2017). "Implementation of additional training profiles «LETI minor»: Using online courses," 2017 IEEE VI Forum Strategic Partnership of Universities and Enterprises of Hi-Tech Branches (Science. Education. Innovations) (SPUE), St. Petersburg, 2017, pp. 147-148, doi: 10.1109/IVForum.2017.8246076.

[20] R. D. Costa, G. F. Souza, T. B. Castro, R. A. M. Valentim and A. P. Dias, (2020). "Identification of Learning Styles in Distance Education Through the Interaction of the Student with a Learning Management System," in IEEE Revista Iberoamericana de Tecnologias del Aprendizaje, doi: 10.1109/RITA.2020.3008131.

[21] Alexandrovna, S. T. (2018). "The Role of Distance Educational Technologies in the Development of Educational Programmes in a Network Form: Experience and Relevant Problems," 2018 IV International Conference on Information Technologies in Engineering Education (Inforino), Moscow, 2018, pp. 1-4, doi: 10.1109/INFORINO.2018.8581847.

[22] Simonson, M., Smaldino, S., Albright, M., & Zvacek, S. (2003). Teaching and learning at a distance (2nd ed.). Upper Saddle River, NJ: Merrill Prentice Hall.

[23] Zirkle, C., & Shoemaker, H. (1999). Indiana State's multiple delivery approach: Integrating industrial technology education with educational technology. The Technology Source. Retrieved March 27, 2003, from http://www.mivu.org/teaching/techsource/

[24] Zirkle, C. (2000). Preparing technical instructors through multiple delivery systems: A working model. T.H.E. Journal 28, (4), 62-68.

[25] Aydın, C., C.; Tirkes, G. (2010). Open Source Learning Management Systems in E-Learning and Moodle, Atilim University, Ankara: Turkey.

[26] Perales, M., Pedraza, L. and Moreno-Ger, P. (2019). "Work-In-Progress: Improving Online Higher Education with Virtual and Remote Labs," 2019 IEEE Global Engineering Education Conference (EDUCON), Dubai, United Arab Emirates, 2019, pp. 1136-1139, doi: 10.1109/EDUCON.2019.8725272.

[27] Szőke, J. and Kecskés, P. (2017). "Virtual proximity in distance education — The usage of a three-dimensional software," 2017 8th IEEE International Conference on Cognitive Infocommunications (CogInfoCom), Debrecen, 2017, pp. 000529-000529, doi: 10.1109/CogInfoCom.2017.8268291.

[28] M. Maravanyika, N. Dlodlo and N. Jere, "An adaptive recommender-system based framework for personalised teaching and learning on e-learning platforms," 2017 IST-Africa Week Conference (IST-Africa), Windhoek, 2017, pp. 1-9, doi: 10.23919/ISTAFRICA.2017.8102297.

[29] Yun Wu, W., Weng, K., Wen, M., You, B. and Lian, J. (2017). "The Construction of Web-Learning System and Learning Performance Based on Online Interaction and Self-Regulation Theories-Architectural Design Curriculum," 2017 *International Conference on Information, Communication and Engineering (ICICE)*, Xiamen, 2017, pp. 288-291, doi: 10.1109/ICICE.2017.8479001.

# Propagation Measurements and Pertinency of Models for Communications Systems in Oman

Zia Nadir
ECE Department, Sultan Qaboos University
nadir@squ.edu.om

Hassan Al Lawati
ECE Department, Sultan Qaboos University
hlawati@squ.edu.om

Mahmood Al Rashdi
Omantel
alrashdi.mahmood@gmail.com

***Abstract*—This article discusses the usefulness of Okumura-Hata model and Sakagami model in urban areas for 2G and 3G communication systems. At some places, applicability of the models (Okumura Hata and Extended Sakagami) is studied and extended to a much lower distance from the tower than the specified minimum distance indicated in the model. Authors did an extensive drive test in urban areas and post also processed data and proposed theoretical modified model which is presented and compared for different data sets at different locations in Oman. Higher order interpolating polynomial was also used which helps in reasonable prediction for RF engineers.**

***Keywords—Propagation Models, Okumura Hata, Sakagami, Pathloss.***

## I. Introduction

It is very challenging for wireless network designers to estimate the pathloss of transmitted signals to ensure the quality of service. Generally, the wireless signal is impacted by a variety of propagation mechanisms. These mechanisms include signal reflection, diffraction and scattering. Considering the GSM as the second mobile generation (2G) globally spread RF technology, many propagation models study the pathloss and predict the signal strength at specific distance by predicting the Maximum Permissible Loss (MPL).

This paper is an extension to a paper published recently at IEMTRONICS 2020 of same authors (Rashdi, Nadir, & Lawati, 2020). However, current paper tackles also another model (Sakagami) and additional paths for experimental data in analysis. This paper proposes and focuses on the urban area with its extension in order to have a suitable propagation model for this area or any other urban area. The Okumura-Hata has been practiced before by several researchers and compared to the real measured data. The Root Mean Square Error (RMSE) is to be used as one indicator as an error indicator and results validator. Okumura-Hata model also needs to be studied for 3G frequency spectrum to provide lower RMSE value which are not done before in these areas. Then, the generalized equation has to be obtained by averaging the RMSE values for studied paths in each area. The generalized formulas than is to be tested and verified in different paths of other areas and the obtained results should be within expected range (Jianhui & Dongfeng, 1998).

For several factors, the RF design is a highly challenging. Special efforts are required in order to provide good coverage with sufficient capacity which satisfies the high demands of this populated area. Hence, the path loss variation with respect to distance is investigated and studied in this work. This is very helpful for RF engineers in order to have a special propagation model that can assist the radio network planners to implement high efficient network. In a radio communication system, the pathloss exponent has a solid effect on the quality of signals. Accordingly, it is required to precisely estimate or predict a perfect design of radio communication network.

There are several researchers who working in this area. Several research findings are linked or address modelling of pathloss effects for a very narrowband communication by using diverse techniques starting from analytical models to empirical models. Businesses in this area are having a major issue to get maximum received power. So, for them losses that occur during transmission of signals from the transmitter to the receiver is very critical. This work addresses, the empirical method along with other techniques. It is tedious as it involves the huge data collection, analysis and processing and performing drive test. A fixed distance was initially taken from the base station to the receiver and later drive test was conducted. As a first step, the Centre of Business District (CBD) area has been subdivided into two sub areas. The reason for this is to facilitate the study in terms of data analysis and manipulation. Also, it has to be mentioned that each area differs from each other slightly in terms of buildings pattern arrangement. The buildings of the main area are quite tall and aligned in a uniform pattern. On the other hand, the buildings of the extended area are comparatively shorter and closer to each other. For the purposes of path loss modelling study, a GSM site in each of the two areas has been selected to be used as an RF signal transmitter. The name chosen for the site in the area is 'Path-1 and Site-1' and that for the extension area is 'path-3 and Site-1'.

Copyright © AJSE Publishers 

## II. Propagation Models

### A. Free Space Propagation Model

As there is an increase in frequency, further to it, rapidly received signal decreases its amplitude when we increase over distance. Due to this reason, some companies like to use 700Mhz for their cell-phones. This can cover a larger distance. WiMAX service, in the 2.5 GHz band loses power more quickly over distance than 700MHz. Similarly, some services in 5800MHz and above lose power even more intensely when distance is increased. This forces the operators to use higher power levels and big high gain antennas which has additional challenges. These figures are not yet in dB which has the effect of reducing the exponential signal deterioration over distance into a straighter graph. The pathloss, which represents signal reduction as a positive quantity measured in dB, is defined as the difference (in dB) between the effective transmitted power and the received power, and may or may not include the effect of the antenna gains. The free space power received by an antenna separated from a transmitter antenna by a distance d, is given by Frii's free space equation (1):

$$P_R(d) = \frac{P_t G_T G_r \lambda^2}{(4\pi)^2 d^2 L} \tag{1}$$

Pt is the conveyed power, Gt , Gr are the Gain of the source and receiver respectively, $\lambda$ is the wave length(m), d is the distance between source and receiver and L is the system loss factor ($L \geqslant 1$). The free-space pathloss denoted by Lp(d) is given by equation (2):

$$L_P(d) = \left(\frac{\lambda}{4\pi d}\right)^2 \Rightarrow L_P(dB) = -20 \log_{10}\left(\frac{\lambda}{4\pi d}\right)$$
$$\because L_P(d) = 20\log_{10} f_C + 20\log_{10} d - 147.56\,[dB]$$

(2)

It can be seen from (2) that the free-space pathloss increases by 6dB when doubling the distance.

### B. Urban Propagation Environment

There are several parameters which contribute in the propagation mechanisms. The signal is affected as it moves through an urban environment. There are structures, constructions which cause the signals to be returned or diverted and scattered. These phenomena of propagation of radio signals can be caused by Trees and foliage. The reduction of signals strength, can be measured by taking the difference between the median signal levels in front of the building and inside the building. We can go into depth by taking into account the civil engineering aspects of the buildings, materials used etc. In this case we can be more precise in prediction. Reflection, diffraction, and scattering are the three basic propagation mechanisms which impact propagation in a mobile communication system.

### C. Plane Earth Propagation Model

Propagation representations are scientific depiction of results of tests carried on the propagation of wave under several different frequencies, antenna heights and locations over different periods and distances. When the radio wave propagates over the ground, it can be partially absorbed and the rest is reflected back to the medium. Due to the reflection from earth surface, the power of the signal can be higher than predicted by the free space model. Pathloss intended for the plane Earth Model is shown in (3 and 4)

$$P_r = P_t\, 20\left(\frac{h_1 h_2}{d^2}\right) \tag{3}$$

$$L_p = -10\, Log_{10}\, P_t\, 20\left(\frac{h_1 h_2}{d^2}\right)^2 [dB] \tag{4}$$

Where, (d) = the path length (m)

($h_1$) = BS height (m)

($h_2$) =MS height (m).

We have to select another model due to its limitations for GSM. Model should also consider, all other aspects also e.g. reflections from buildings, multiple propagation or diffraction effects. Further, due to changes in $h_2$, everything will change and prediction or measurements will not be accurate.

### D. Attenuation Factors

Ideally in free space the signal would be sent and received with no loss but that is not the case in reality. As the signal propagates through the medium, it encounters obstacles that contribute in the attenuation of the signal power. Hence, interpreting their contribution in the pathloss equations is necessary. The weather factors are too many and for simplicity they are often neglected. Due to this neglecting, the calculations will encounter some error. To achieve better accuracy, these factors are inserted into the model as RMSE. Rain is one of the attenuation factors. An area with high rain rate would encounter more attenuation than an area with no rain. This attenuation might be expected due to the nature of the rain drop. The rain drop is the result of a condensed water steam at low temperature. Due to its nature, the rain drop might scatter, absorb or reflect the signal. Humidity is another attenuation factor that contributes to the pathloss. The humidity is the result of the evaporation of water in the atmosphere near earth. Areas like coasts are high humidity areas. The attenuation encountered due to humidity in such areas is expected to be higher than areas with low humidity.

## III. Empirical Models

Propagation models are elaborated in this section; between them are Okumura-Hata model which was finally adopted for this article.

### A. Okumura Model

Okumura's model is one of the most widely used models for signal prediction in urban areas. This model was the result of intensive propagation tests for mobile systems at different frequencies conducted by a Japanese scientist called Okumura. This model is represented by a set of curves (frequency (MHz) verses attenuation (dB)) assuming mobile antenna height of 3m. This model is appropriate under the following circumstances:

- Frequency range of 150-1920MHz,
- Distance from BTS of 1-100km,
- BTS height of 30-100 m.

*B. COST231 Model*

This model is a modification of Okumura-Hata model. The extension of this model includes higher frequencies which were not covered by the Okumura-Hata model.

*C. Walfisch Model*

This model was developed by Walfisch and Bertoni. It considers the impact of rooftops and building height by using diffraction to predict average signal strength at street level.

*D. Okumura-Hata Model*

Hata's model is the extension of Okumura's. This model can be similar to a mathematical illustration of the Okumura's model. It's in the form of empirical formulas. This model is consistent with the Okumura model for distances greater than 1km. The conditions or basic limitations for this are mentioned as below:

- Frequency range of 150-2000MHz,
- Distance from BTS of 1-100km,
- BTS height of 30-200m,
- MS antenna height 1-10m

The limits on this technique is due to range of test outcomes as illustrated above (Jianhui & Dongfeng, 1998). Hata created several typical Pathloss scientific models for different areas e.g. urban, suburban and open country environments, as mentioned in the following equations, respectively. Model takes urban areas as a reference and applies correction factors as mentioned below: For urban areas generalized Okumura-Hata model is given below:

$$L_{dB} = A + BLog_{10}R - E_{1,2,3} \qquad (5)$$

Where:

$$A = 69.55 + 26.16\,Log_{10} f_c - 13.82\,Log_{10} h_b$$
$$B = 44.9 - 6.55\,Log_{10} h_b$$
$$E_1 = 3.2\left(Log_{10}\left(11.7554 h_m\right)\right)^2 - 4.97 \quad for\ cities;\ f_c \geq 300MHz$$
$$E_2 = 8.29\left(Log_{10}\left(1.544 h_m\right)\right)^2 - 1.1 \quad for\ cities;\ f_c \leq 300MHz$$
$$E_3 = \left(1.1Log_{10} f_c - 0.7\right)h_m - \left(1.56\,Log_{10} f_c - 0.8\right)$$
$$for\ relatively\ smaller\ cities.$$

Where:

$h_m$; MS height [m]

$d_m$; distance between the phone and the building [km]

$h_0$; height of a building [m]

$h_b$; BS height [m]

r; circle distance BS and mobile [m]

R=r x 10-3 great circle distance between BS and mobile [km]

$f_c$= frequency [MHz]

Rest of the parameters are as mentioned above for small and medium cities (Z. Nadir, 2012; Zia Nadir & Ahmad, 2010; Wilson & Scholtz, 2003).

*E. Extended Sakagami model*

This model is described in (Shalangwa, D. A., & K., 2010) is presented by following equation:

$$\begin{aligned} L_p[dB] = 101.0 - 7.11\log_{10} W \\ + 7.5\log_{10} H \\ - \left(24.37 - 3.7\left({}^{H}/_{h_b}\right)^2\right)\log_{10} h_b \\ + (43.42 - 3.11\log_{10} h_b)\ \log_{10} d \\ + 20\log_{10} f_c - a(h_m) \end{aligned}$$

Where a($h_m$): correction factor for antenna height ($h_m$).

$$a(h_m)[dB] = 3.2(\log_{10}(11.75 h_m))^2 - 4.97$$

So Pathloss can be calculated using the following equation:

$$L_p(dB) = P_t - P_r \qquad (6)$$

Where Pt is the transmitted power which is equal to 47dB for 2G and 34dB for 3G transmitters and Pr is the received power. The major models used for this study is Okumura-Hata model. Authors contribution is the usage of the model for less than 1km and proposing an interpolated polynomial for RF planners.

## IV. Results and Discussions

An intensive drive test was conducted along all pre-identified paths using TEMS. Furthermore, the positioning information is collected via a GPS antenna. The measured data for each path has been recorded in terms of log files and processed using ACTIX. Google Earth program (not shown here in this paper) was also used to plot the received signal strengths. Duplicate data sets were also cleaned before post processing. After that, the data has been worked upon. This area of CBD can be considered as an urban area. After defining, the study was supported to make an evaluation among the tentative and hypothetical data and the outcome is as shown in following Figures. 1-4:

The results of measured path loss have been used as an input for usage with developed MATLAB scripts in order to plot the measured path loss and the predicted path loss curves as a function of distance. MATLAB is an efficient software for mathematical calculation and data analysis. After that, the variation between measured and predicted results has been obtained using RMSE method which was introduced earlier. The RMSE error indication technique has been used to modify each data set to have improved prediction capabilities. RMSE value combined all known and unknown factors and parameters impacting the path loss amount of the propagated signal. These factors include multipath effects, various propagation mechanisms and different weather conditions e.g., temperature and humidity. The RMSE value has been utilized to establish the modified propagation model for each studied path. After that, the RMSE value has been recalculated for the modified equations.

*Data-Set-A*

$f_c$=935.4MHz; $h_b$=25m; $h_m$=1.5m; H=30; W=20;
RMSE Value for Okumura-Hate Model was 7.3864dB and modified RMSE value after modification of Okumura-Hata model was 5.1321dB which is within acceptable range (Jianhui & Dongfeng, 1998). Following figures (1-4) details the Pathloss and modeling.

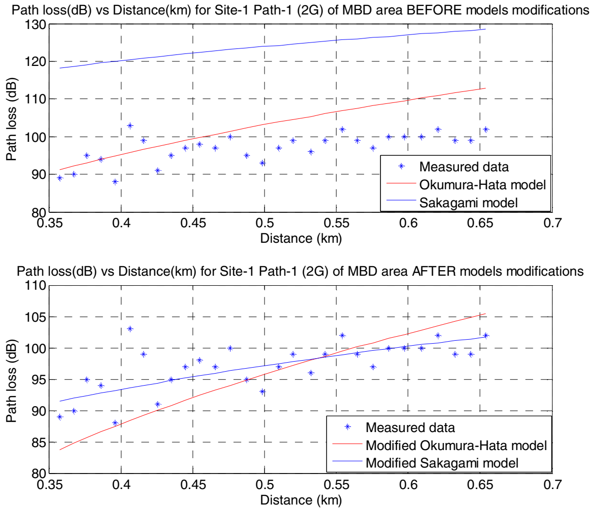


Fig. 1. Experimental and Theoretical Pathloss

RMSE for Okumura-Hata Model is = 7.3864
RMSE for Sakagami Model is = 26.7678
RMSE after modifying Okumura-Hata model is = 5.1321
RMSE after modifying Sakagami model is = 2.9289

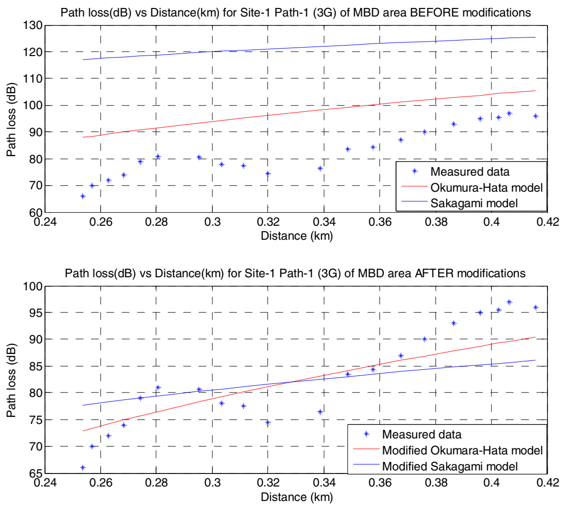


Fig. 2. Experimental and Theoretical Pathloss

RMSE for Okumura-Hata Model is = 15.0821
RMSE for Sakagami Model is = 39.4534
RMSE after modifying Okumura-Hata model is = 4.4799
RMSE after modifying Sakagami model is = 6.7232

*Data-set-B*
$f_c$=2130MHz; $h_b$=28m; $h_m$=1.5m; H=30; W=20;

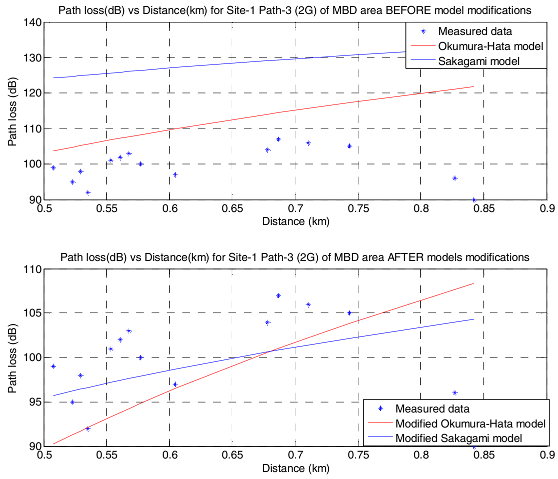


Fig. 3. Experimental and Theoretical Pathloss

RMSE for Okumura-Hata Model is = 13.4640
RMSE for Sakagami Model is = 28.4557
RMSE after modifying Okumura-Hata model is = 7.7247
RMSE after modifying Sakagami model is = 5.5071

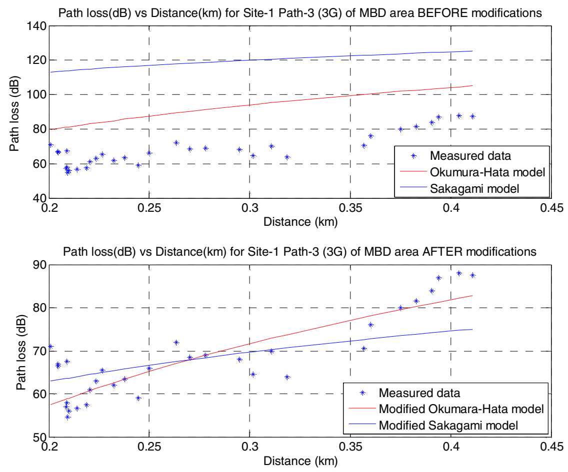


Fig. 4. Experimental and Theoretical Pathloss

RMSE for Okumura-Hata Model is = 22.3003
RMSE for Sakagami Model is = 50.2530
RMSE after modifying Okumura-Hata model is = 5.1666
RMSE after modifying Sakagami model is = 6.3872

Above shown graphs and after comparing with articles (Jianhui & Dongfeng, 1998; Z. Nadir, 2012; Zia Nadir & Ahmad, 2010) the results visibly display that the measured Pathloss is smaller in value than the predicted Pathloss by a variance from 5dB to 20dB. Nevertheless, there are several explanations that may have triggered those substantial modifications. First of all, in Japan there are few zones virtually fulfilling the conditions; and if any, they are narrow. Because of that reason Okumura selected the value for urban area as standard for open areas (Wilson & Scholtz, 2003). Furthermore, the topographical situation of Japan is different from that of our country due to geographical differences. Accordingly, Root Mean Square Error (RMSE) was considered amongst those two different values of pathloss, for Hata model, using following (7) (Jianhui & Dongfeng, 1998) (Shalangwa et al., 2010):

$$RMSE = \sqrt{\frac{\sum_{i=1}^{N}(Pmeasured_i - Pcalc_i)^2}{(N-1)}} \quad (7)$$

N: Measured Data Points

The RMSE acceptable range is up to 6dB so, the RMSE is adjusted with the Hata equation for urban area and the modified Hatas' equation is as given below (8):

$$\begin{aligned} L_{p\_mod}(urban) &= 69.55 + 26.16Log_{10}(f) \\ &- 13.82Log_{10}(h_b) + (44.9 - 6.55Log_{10}(h_b))Log_{10}(d) \\ &\pm MSE - (1.1Log_{10}(f) - 0.7)h_m - (1.56Log_{10}(f) - 0.8) \end{aligned} \quad (8)$$

The modified result of Hata equation is shown in Fig. 5 and Fig. 6 and the RMSE in this case is less than 6dB, which is acceptable (Jianhui & Dongfeng, 1998) .

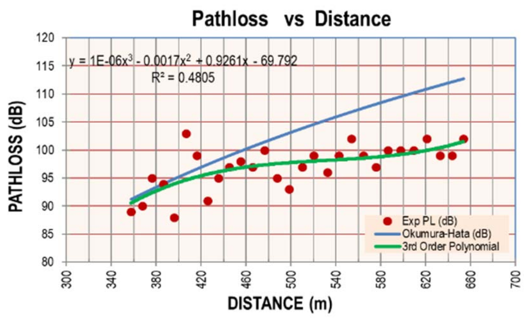


Fig. 5. Theoretical and Exp. Pathloss versus distance for data-set-A

For verification, whether the modified Hata's equation is applicable for some other areas, another data generated from TEMS tool has been used. Based on that practical data, the propagation Pathloss and the distance have been re-verified for (Zia Nadir, Mohamed, & Touati, 2008).

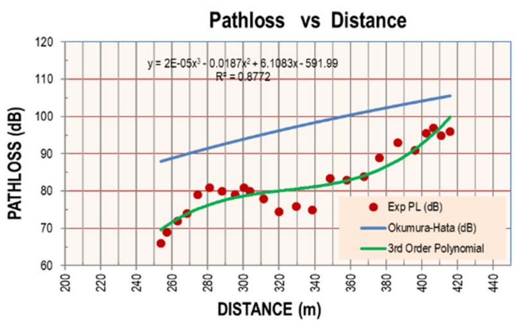


Fig. 6. Theoretical and Exp. Pathloss versus distance for data-set-B

Hypothetical imitation and the found new data are equated and examined further using 3rd order polynomial to interpolate on same experimental data set which provided moderate flexibility. As shown in figures above, higher order polynomial also provides an equally even and effective guess without cumulative computational difficulties, which is expected for these estimates. A decent relationship is detected for the entire series of data set. The decent agreement of the features demonstrate that experimentally replicated numbers is a decent representation of that defined by Hata model.

Additionally, the simulation and the attained tentative data is associated and examined additionally using other models like extended Sakagami model on the set of the new data which gives also satisfactory results. After observation, it can be safely said that the scatter plot of the experimental data on pathloss vs distance reveals a third order polynomial tendency. Fig.5 and Fig. 6 above, show the theoretical, experimental and 3rd order polynomial plots for Okumura-Hata propagation model. As can be seen, results show good agreement between various studies.

Universally, by calculating the RMSE for the second dataset it was also found to be less than 6dB, a satisfactory number. Nevertheless, some experimental values were a bit far from the interpolated points that can be related to the nature of the cell with high rise structures. Though there are many forecasts approaches that are based on deterministic procedures through the availability of improved databases, the Okumura-Hata model is still frequently used (Zia Nadir & Bait-Suwailam, 2014) (Zia Nadir, Bait-Suwailam, & Shafiq, 2014) . We are also aware that the hindrances in the path significantly affect the radio signal propagation (Hrovat, Kandus, & Javornik, 2012). Above all, wireless communication system avoids obstacles such as crossing objects owned by others. There are also many difficulties in establishing a wireless communication system in some applications (L khagvatseren. T & F, 2011). As can be seen from above results, there are some discrepancies between RMSE values for each path compared to the other, although the modified results for each path are within accepted standards. After deep analysis and investigation of the possible reason for this mismatch, it has been noticed that some paths are served by the main lobe of antenna radiation, some are served by side lobes and some are served by a combination of the main lobe and side or back lobes. This conclusion has been obtained by reviewing all paths in Google Earth map with respect to the area of specific serving lobe. The following figure 7 shows general antenna radiation pattern concept and the radiation pattern of another site.

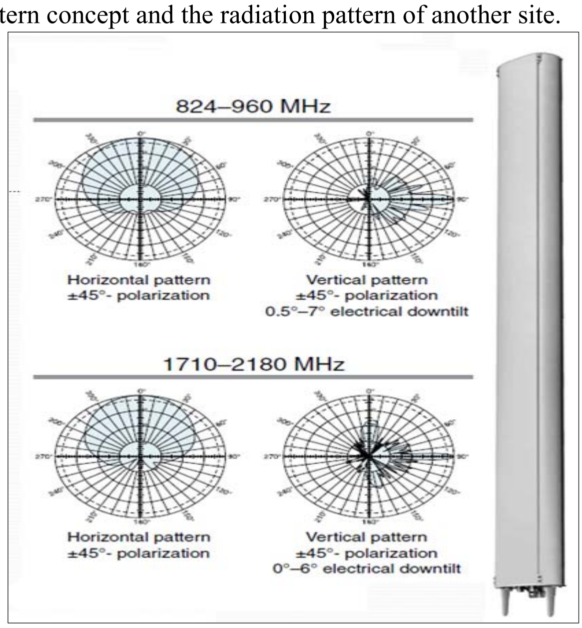


Fig. 7. Radiation pattern of an antenna on one site

In order to produce a generalized model for UMTS path loss prediction use, the average of RMSE for all tested paths was calculated for the model. Then, the same well known process has been applied in to obtain a generalized equation for the propagation model. After that, these equations have been applied for three different paths but not shown here. They are namely: Site-1 Path-1, Site-1 Path-3 respectively. The MATLAB programs for each path was developed and used for generalization and further verification.

This work can be considered as a step forward in establishing generalized propagation models used for path loss prediction in other urban cities of Oman. Further intensive and comprehensive studies and research is recommended to achieve this goal. Also, it is highly recommended to incorporate various modelling techniques in addition to the RMSE method to study their accuracy and impact. Moreover, it is recommended to include more parameters in future prediction models that impact the signal propagation e.g., antenna parameters and patterns.

## V. Conclusion

As mentioned earlier, this paper is an extension to a paper published recently at IEMTRONICS 2020 of same authors. However, current paper tackled also another model (Sakagami) and additional paths for experimental data in analysis. This study focused on forecasting the root mean signal strength in diverse areas. As utmost propagation models aim to forecast the median pathloss, existing prediction models vary in terms of their applicability over different terrain and environmental conditions. The effects of terrain situation predicted at 900MHz and 2.1GHz were analyzed. Experimental outcomes of radio signals propagation for an urban area in Oman were related with those predicted based on Okumura-Hata model. The contribution is the prediction by at lower distances than the model is generally used and also validation of experimental data. If precise environmental information was included in the model, better prediction results might be achieved. 3$^{rd}$ order polynomial gave us also the unavailable experimental points showing a good agreement within adequate boundaries.

## Acknowledgment

The authors would like to thank SQU and Omantel for their support for this study.

## References

Hrovat, A., Kandus, G., & Javornik, T. (2012). Path loss analyses in tunnels and underground corridors. *International journal of communications, 6*, 136-144.

Jianhui, W., & Dongfeng, Y. (1998, 8-11 Sept. 1998). *Propagation measurements and modeling in Jinan city.* Paper presented at the Ninth IEEE International Symposium on Personal, Indoor and Mobile Radio Communications (Cat. No.98TH8361).

L khagvatseren. T, & F, H. (2011). Path loss aspects of a wireless communication system for sensors. *INTERNATIONAL JOURNAL OF COMPUTERS AND COMMUNICATIONS (NAUN), 5*(1).

Nadir, Z. (2012, 11-13 Jan. 2012). *Empirical pathloss characterization for Oman.* Paper presented at the 2012 Computing, Communications and Applications Conference.

Nadir, Z., & Ahmad, M. (2010). Characterization of Pathloss Using Okumura□Hata Model and Missing Data Prediction for Oman. *AIP Conference Proceedings, 1285*, 509-518. doi: 10.1063/1.3510574

Nadir, Z., & Bait-Suwailam, M. (2014). *Pathloss Analysis at 900 MHz for Outdoor Environment*. Paper presented at the International Conference on Communications, Signal Processing and Computers (EUROPMENT 2014 ), Interlaken, Switzerland.

Nadir, Z., Bait-Suwailam, M., & Shafiq, M. (2014). RF Coverage Analysis and Validation of Cellular Mobile Data using Neural Network. *INTERNATIONAL JOURNAL of NEURAL NETWORKS and ADVANCED APPLICATIONS, 1*, 30-36.

Nadir, Z., Mohamed, N., & Touati, F. (2008). Pathloss Determination using Okumura-Hata Model and Spline Interpolation for missing Data for Oman. *Lecture Notes in Engineering and Computer Science, 2170*.

Rashdi, M. A., Nadir, Z., & Lawati, H. A. (2020). *Applicability of Okumura – Hata Model for Wireless Communication Systems in Oman*. Paper presented at the International IOT, Electronics and Mechatronics Conference (IEMTRONICS 2020), Vancouver, Canada. https://iemtronics.org/

Shalangwa, D. A., S., & K., S. (2010). Measurement and modeling of pathloss for GSM900 in sub urban environment over Irregular terrain. *IJCSNS International Journal of Computer Science and Network Security*.

Wilson, R. D., & Scholtz, R. A. (2003, 1-5 Dec. 2003). *Comparison of CDMA and modulation schemes for UWB radio in a multipath environment.* Paper presented at the GLOBECOM '03. IEEE Global Telecommunications Conference (IEEE Cat. No.03CH37489).

Copyright © AJSE Publishers 

# A Comparative analysis of Maximum Power Point Tracking Techniques for Battery Operated PV Systems at Different Temperatures

**Pankaj Sahu**[1]
Research Scholar (Ph.D.)
Dept. of ECE, SoET,
BML, Munjal University,
Gurugram, India

**Ashish Sharma**[2]
Student,
Dept. of ECE, SoET,
BML, Munjal University,
Gurugram, India

**Dr. Rajiv Dey**[3]
Assistant Professor,
Dept. of ECE, SoET,
BML, Munjal University,
Gurugram, India

***Abstract*—This paper presents a comparative analysis of Ripple Correlation Control (RCC) with conventional Maximum Power Point Tracking (MPPT) methods such as Perturb & Observe (P&O) and Incremental Conductance (IC). Photovoltaic (PV) array along with the buck converter and its MPPT control have been simulated for all three MPPT methods at different solar radiation levels at 25°C and 70°C and results have been compared. From the simulation results, it can be observed that P&O is much affected with slow tracking and oscillations, and IC MPPT performs better than P&O in terms of tracking, but not for ripples. Simulation results verifies that RCC MPPT is capable of solving both these problems effectively and RCC performance is better than both P&O and IC MPPT methods.**

***Keywords—PV, MPPT, RCC, HC, P&O, IC.***

## I. Introduction

Sustainable energy resources are always in high demand due of the fast and continuous depletion of fossil fuels and oil resources. Among the available green energy resources, solar energy has emerged as one of the most impactful renewable energy resources which has the potential to replace conventional energy sources. Solar energy is a free and constant source of renewable energy which is harvested using environment-friendly photovoltaic systems. However, it also suffers from some drawbacks e.g. during the day time, level of solar insolation is non uniform, moreover, increase in the environmental temperature degrades the power transfer to the load. Therefore, the power generated by solar panel is not same all the time and due to this each and every time the Maximum Power Point (MPP) of photovoltaic system gets changed [1]. Solar panel can deliver maximum power to the load for a certain value of voltage $V_{MP}$ and current $I_{MP}$. This point is known as Maximum Power Point (MPP) as shown in Figure 2.

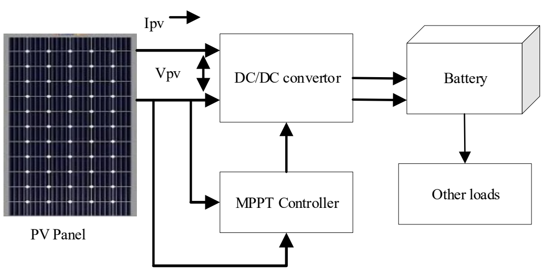


Fig. 1. Single stage battery operated PV system.

Since, the output power generated per watt by solar panel is too high, it is reasonable to improve its performance via power converters. These converters have many advantages in solar PV system like it can provide isolation between PV panel and load, extract maximum power. Moreover, converters are effective means for implementing MPPT technology [19]. MPPT algorithms are integrated with power electronic converter which can deliver maximum power by controlling its duty cycle. In Photovoltaic systems MPPT based charge controller is preferred over PWM as a typical PWM charge controller can only be able to regulate the output voltage of a Photovoltaic (PV) array, not the current, but in MPPT controller both the voltage and current can be regulated. A general block diagram of a battery-operated PV system is shown in Figure 1.

Many research works have been done on MPPT in the last few decades such as conventional methods like Perturb and Observe [1-10], Incremental Conductance [11-16], Hill Climbing [17-19] have been deployed and a large number of modifications for these techniques has been proposed in the literature. The main shortcomings of P&O, HC & IC is that these methods can only track the maximum power when the irradiation conditions are uniform and it fails to track MPP when there is a partial shading or cloudy environmental condition. Further, these methods suffer from poor convergence, slow tracking speed, and high steady state oscillations (ripples). Therefore, to track the MPP under partial shading conditions conventional methods need to be modified. Due to which different modified versions of P&O have been proposed in the literature such as Adaptive P&O with fixed step size, variable step size, etc. [2-3]. Additionally, Soft Computing/Evolutionary algorithms [19] based approaches have also been emerged along with the conventional MPPT methods such as particle swarm optimization based MPPT algorithm [20] which is useful in finding the global MPP when there are multiple PV array with large area. These methods have numerous advantages like (i) ability to handle non linearity (ii) wide exploration in search space and (iii) coherent skill to reach global optimal regions these methods is considered to be a prime choice for non-linear optimization. Even-though the above alterations have enhanced the performance of MPPT charge controllers however, it is not sufficient enough for all the environmental conditions [6, 12]. This gives a motivation to the researchers to find some alternative ways to improve the performance of MPPT charge controllers under partial shading conditions.

Copyright © AJSE Publishers

On the other hand, new era of MPPT algorithms in PV system have emerged when evolutionary algorithm was first applied for MPP tracking [21-22]. Due to its ability of handle nonlinear problems it has opened up new scopes of opportunities due to its simplicity, robustness and ripple removal characteristics. Ripple Correlation Control (RCC) [21-26] provides a solution to the steady state oscillations, which is mainly caused by the internal ripples present in the system due to the presence of power electronic circuitry. Since, P&O, IC, and HC methods do not consider these ripples as internal perturbations, due to which the algorithm consider them as external perturbations. As a result the output voltage and current oscillates around MPP, in turn power also oscillates. These oscillations are harmful for the battery, as it reduces its operating life span.

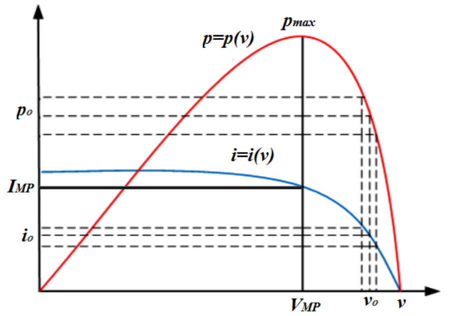


Fig. 2. Current and power of the PV panels versus voltage.

In this work, RCC MPPT with buck converter for battery connected load has been implemented and its simulation results have been compared with P&O and IC MPPT methods. This work is an extension of [27]. The organization of the paper is as follows; Section I gives introduction of MPPT and various existing methods available in literature. Section II provides mathematical formulation of P&O, IC and RCC method, along with formulation of buck converter used in the simulation. In section III, parameters specifications are given along with photovoltaic system diagram. Section IV is simulation results and discussion, followed by conclusion in section V.

## II. Back Ground of the Conventional MPPT Methods

In this section, a brief overview of the conventional MPPT methods along with detailed explanation of RCC control algorithm has been discussed.

### *A. Perturb & Observe (P & O)*

The P&O Method [1-10] utilizes additional perturbations of current or voltage array to check if the system has achieved the nominal value of voltage or current. If the power output increases when voltage is changed in a particular direction of perturbation then it means that MPP will be obtained in that particular direction of perturbation and if the power output decreases for the same voltage perturbation then the MPP can be found by reversing the direction of perturbation. Although this method is easy to implement and is cost effective the overall system is never able to attain stability because apart from adding external perturbation to it the perturbation due to the environmental changes and the inherent generated perturbation affects its stability.

This method works on concept of continuous observations of PV array output power for the input perturbations, due to changing current or voltage of PV array. The algorithm continuously modifies the reference voltage or current based on the previous value of power until reaches the MPP [6, 7]. When $dP/dV > 0$ and the operating voltage of PV array is perturbed in a specific direction, it known that perturbation moves the operating point of PV array to the MPP. P&O method will then continue to perturb the PV voltage in the same direction. When $dP/dV < 0$, the perturbation moves the operating point of PV array away from the MPP and the P&O method reverses the direction of the perturbation [8, 9].

### *B. Incremental Conductance (IC)*

Another algorithm to locate the MPP is Incremental Conductance (INC) [11-16]. In this algorithm a relationship between power and voltage is established where ideally the derivative of power with voltage is zero. This algorithm has both hardware and software complexity and is also expensive. The main drawback of this algorithm is that it increases the computation time of MPPT

$$\frac{dP}{dV} = \frac{d(VI)}{dV} = I\frac{dI}{dV} + V\frac{dI}{dV} = I + V\frac{dI}{dV} \ . \qquad (1)$$

Equation 1 represents the derivative of PV output power with voltage, the PV system will operate at MPP when this equation is equal to zero i.e.

$$\frac{dP}{dV} = 0 \Rightarrow I + V\frac{dI}{dV} = 0 \Rightarrow -\frac{I}{V} = \frac{dI}{dV} . \qquad (2)$$

Comparing the instantaneous change in conductance, $dI/dV$ and instantaneous conductance of PV array I/V in equation 2, the position of operating point in relation to maximum power point can be revealed. Equation 3 shows the position of operating point at different values of $dP/dV$

$$\begin{cases} \frac{dP}{dV} > 0, for\ V < V_{MPP} \\ \frac{dP}{dV} = 0, for\ V = V_{MPP} \\ \frac{dP}{dV} < 0, for\ V > V_{MPP} \end{cases} \cdot \qquad (3)$$

### *C. Ripple Correlation Control (RCC)*

Ripple correlation control is a nonlinear control approach applicable to power electronic circuits. It makes use of voltage, current, or power ripple and correlates this with switching functions to affect control [22]. The RCC solves major problems through less complex implementation. The most important factors and advantages of the RCC are the simple circuit implementation, fast computation/simulation time, there is no need for external perturbation like in P&O and IC, to generate ripple contents, converges asymptotically to the object and its converging rate can be tuned by the controller gain [21]. RCC is a method that is used to calculate the duty cycle which provides maximum power, which will be supplied to the gate of switching circuits to maintain MPP. The main advantage of RCC is that it uses inherent ripples that occur due to the power electronic elements i.e., the DC-DC convertor used in the PV system. Through the correlation of the time based derivative of voltage and power the RCC tries to identify whether this correlation is greater than zero i.e., to the left of the MPP, or less than zero i.e., to the right of the MPP, or exactly zero i.e., equal to MPP.

$$\frac{dp_{PV}}{dt}\frac{dv_{PV}}{dt} > 0\ when\ V_{PV} < V_M, \qquad (4)$$

$$\frac{dp_{PV}}{dt}\frac{dv_{PV}}{dt} < 0 \; when \; V_{PV} > V_M, \quad (5)$$

$$\frac{dp_{PV}}{dt}\frac{dv_{PV}}{dt} = 0 \; when \; V_{PV} = V_M. \quad (6)$$

The general equation used to find the ripple content is as: $\tilde{x}(t) = x(t) - \bar{x}(t)$ (7)

$x(t)$ is the general quantity that can be array current, voltage or power which contains both the ripple as well as moving average component. $\tilde{x}(t)$ is the ripple content whereas $\bar{x}(t)$ is the average component. From equation (7) we can easily find out the ripple content of voltage, current and power.

Figure 3 represents the RCC that has been implemented to find out the duty cycle. This RCC is different from [21-22], as it has low pass filter instead of high pass filters as in [21-22]. In this work RCC mentioned in [25] is implemented for battery operated systems for output power of 95 watts. The work differs from [25], in terms of load which is battery in this work and converter type, which is buck converter, instead of boost converter used in for grid connected load as in [25]. From the Figure 3 error is equal to the product of the ripple content of both the power and voltage.

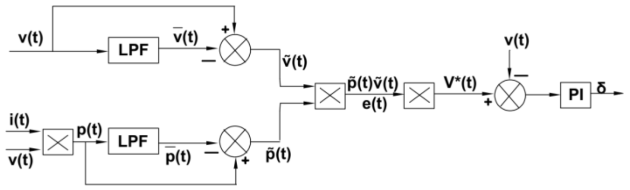


Fig. 3. RCC block of the MPPT Controller

To obtain the error $e(t)$ of power we will use the following mathematical equations;

$p(t) = v(t) \times i(t)$ (8)

Expressing i(t) and v(t) in terms of their ripple content as in (7) and using them in (8) we get,

$$p(t) = \bar{v}(t) \times \bar{\imath}(t) + \bar{\imath}(t) \times \tilde{v}(t) + \bar{v}(t) \times \tilde{\imath}(t) + \tilde{v}(t) \times \tilde{\imath}(t) \quad (9)$$

Therefore, power ripple can be expressed as;

$$\tilde{p}(t) = \bar{\imath}(t) \times \tilde{v}(t) + \bar{v}(t) \times \tilde{\imath}(t) + \tilde{v}(t) \times \tilde{\imath}(t) \quad (10)$$

We can further express the product of $\tilde{p}(t)$ and $\tilde{v}(t)$ as follows;

$$\tilde{p}(t) \times \tilde{v}(t) = \tilde{v}^2(t)\left[\bar{\imath}(t) + \bar{v}(t)\frac{\tilde{\imath}(t)}{\tilde{v}(t)}\right] + \tilde{v}^2(t)\tilde{\imath}(t) \quad (11)$$

Upon taking the derivative of $p(t)$in equation (21) w.r.t. $v(t)$ we get;

$$\frac{dp(t)}{dv(t)} = i(t) + v(t)\frac{di(t)}{dv(t)} \quad (12)$$

Linearizing, Figure 2 at point $v_0, i_0$,we get;

$$\left(\frac{di(t)}{dv(t)}\right)_{v_0} = \frac{\tilde{\imath}(t)}{\tilde{v}(t)} \quad (13)$$

Using equation (12) and (13) error can be expressed as;

$$\tilde{p}(t) \times \tilde{v}(t) = \tilde{v}^2(t)\left[\frac{dp(t)}{dv(t)}\right] + \tilde{v}^2(t)\tilde{\imath}(t) \quad (14)$$

Error is directly proportional to the magnitude of $dp/dv$ as the average value $\tilde{v}^2(t)\tilde{\imath}(t)$ is zero over a cycle, $e(t)$ represents the distance from the MPP. When the output is on the left of MPP the average value of error is positive. When output is on the right of MPP the average value of error is negative. When the output is at the MPP the average value of error is zero. From Figure 3, it can be inferred that when the error signal passes through the first PI controller it generated the reference signal, and the difference of this reference signal & PV array voltage $v(t)$, acts as an input for the second PI controller that gives us the load angle δ, which is used to generate the PWM signal to control the switching of buck convertor.

The DC-DC converter is used to convert one level of DC voltage into another level. According to the requirements one can opt Boost, Buck or Buck-boost converter. In this work a DC-DC buck converter has been used [26]. The primary function of the buck converter is to decrease the voltage according to battery charging requirements with increase in the current for fast charging of battery.

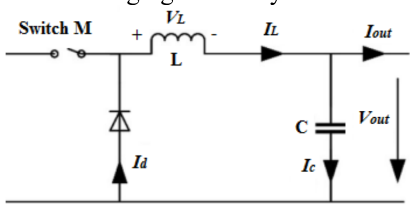


Fig. 4. Electrical Model of DC-DC Buck Converter.

## III. Simulink Model of PV System with RCC MPPT

The Simulink model schematic of the PV system that is used for simulations is depicted in Figure 4, and represents a PV solar panel connected to a resistive load through a dc-dc buck converter with a variant subsystem of MPPT controller that allow to choose between these three MPPT algorithms. P&O, incremental conductance and RCC.

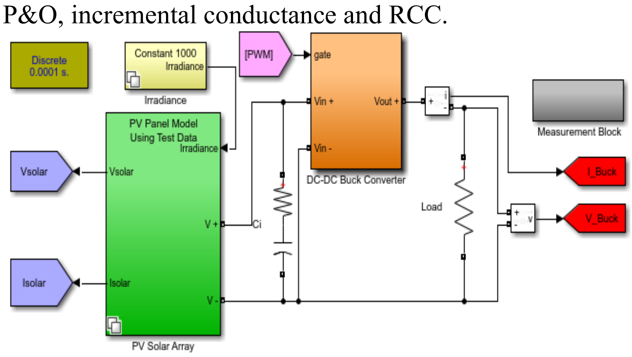


Fig. 5. Simulink Model of PV System.

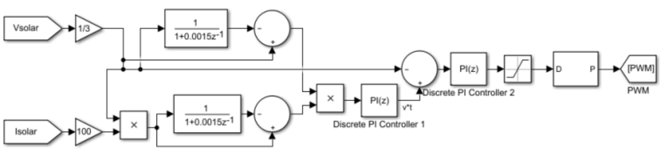


Fig. 6. MPPT variant blocks and Simulink implementation of RCC MPPT controller [25].

The PV parameters used in Simulink simulation model of this work are given in Table I. The components parameters of the buck converter used in Simulink are given in Table II. The components parameters of RCC block are given in Table III.

TABLE I

PV array specifications

| S.No. | Parameter Name | Value |
|---|---|---|
| 1 | Number of cells in series | n-cells = 36 |
| 2 | Open circuit voltage | $V_{oc}$= 21.6 V |
| 3 | Short circuit current | $I_{sc}$= 7.34 A |
| 4 | Series resistance of PV model | $R_s$= 0 Ω |
| 5 | Parallel resistance of PV model | $R_p$= ∞ Ω |
| 6 | Diode quality factor of PV model | $N$=1.5 |
| 7 | DC link capacitor | $C_{dc}$= 100 μF |

TABLE II
BUCK CONVERTER COMPONENTS PARAMETERS

| S.No. | Parameter Name | Value |
|---|---|---|
| 1 | Inductance | $L = 23\ \mu H$ |
| 2 | Capacitance | $C = 120\ \mu F$ |
| 3 | Switching Frequency | $f_{sw} = 2*10^6$ |
| 4 | Sample Time | 0.0001 SEC |
| 5 | Diode Resistance | $R_{ON} = 0.001\Omega$ |

TABLE III
RCC COMPONENTS PARAMETERS

| S.No. | Parameter Name | Value |
|---|---|---|
| 1 | Time constant of LPF's | 1.5 ms |
| 2 | PI controller (inside MPPT block) | $K_p = 200$ |
| | | $K_I = 5.5$ |
| 3 | PI controller (outside MPPT block) | $K_p = 2e\text{-}9$ |
| | | $K_I = -0.009$ |

Simulation has been performed for three different types of variations, fist one is at 1000 W/m$^2$ at 25$^o$C, second at 800 W/m$^2$ at 25$^o$C and third is for step variation [5] as shown in Figure 7.

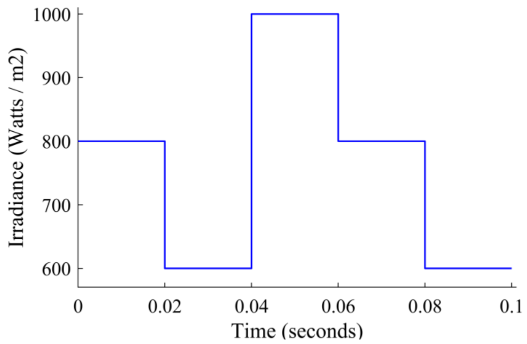


Fig. 7. Step Variation of irradiance [5].

## IV. RESULTS AND DISCUSSIONS

All the simulations have been performed in MATLAB/SIMULINK 2018. First the irradiation level is fixed at 1000 W/m$^2$ at 25$^o$C and 70$^o$C, and results of voltage, current and power for all three methods i.e. perturb & observe, incremental conductance and ripple correlation control have been captured using measurement scopes. Then same process is performed for 800 W/m$^2$ irradiance level at 25$^o$C and 70$^o$C. After this simulation is performed for Step variation of irradiance as shown in Figure 7, and graph were captured. There are many research papers available of P&O and IC methods in which simulation results have been given. In this work PV model parameters have been selected as in [5], since it was also a battery connected system. This work is an extension of [27].

Figures 8, 9, and 10 shows the simulation output of P&O MPPT obtained by the simulation using the setup mentioned in figure 5. The simulation results show that conventional P&O MPPT is very much affected from being slow tracking and oscillations both. This is because of internal ripples, which are generated due to the use of power electronics components. Actually, the system in P&O case, never achieved stability, and it always oscillate around MPP point. It is due to the internally generated ripples, which are considered as perturbations in P&O MPPT. Hence, the performance of conventional P&O MPPT is not up to the mark in terms of stability, ripples and tracking.

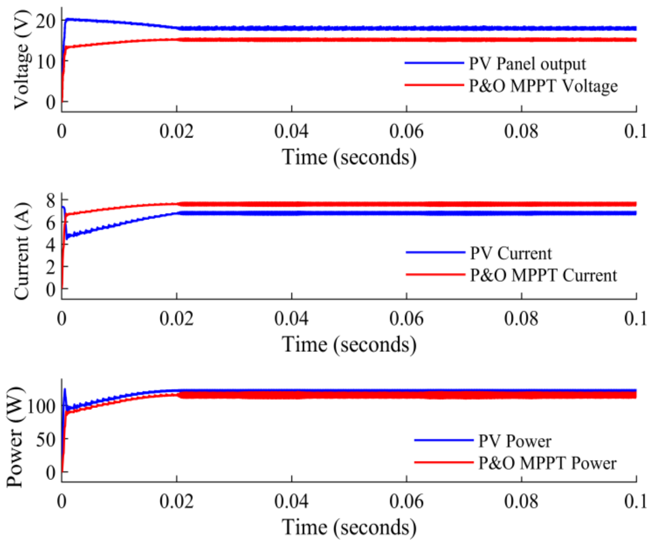


Fig 8. Voltage, Current and Power output of P&O MPPT for 1000 W/m$^2$ irradiance level at 25$^o$C.

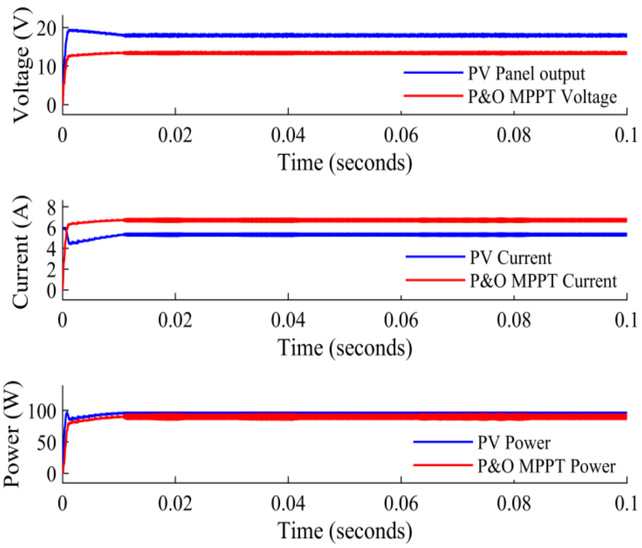


Fig 9. Voltage, Current and Power output of P&O MPPT for 800 W/m$^2$ irradiance level at 25$^o$C.

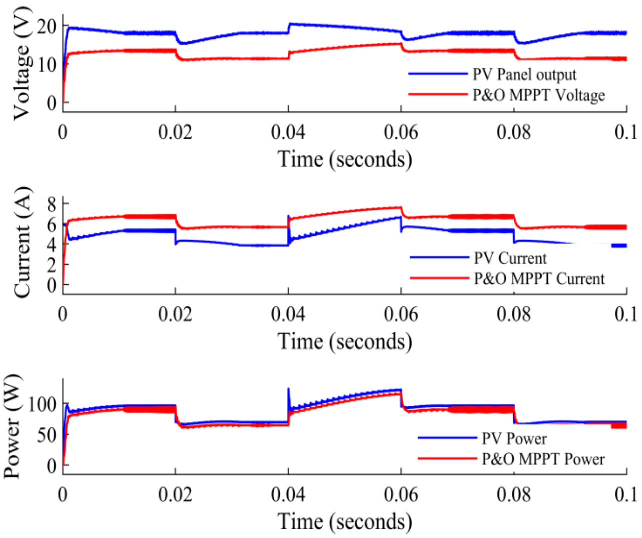


Fig 10. Voltage, Current and Power output of P&O MPPT for Step irradiance at 25$^o$C.

Copyright © AJSE Publishers

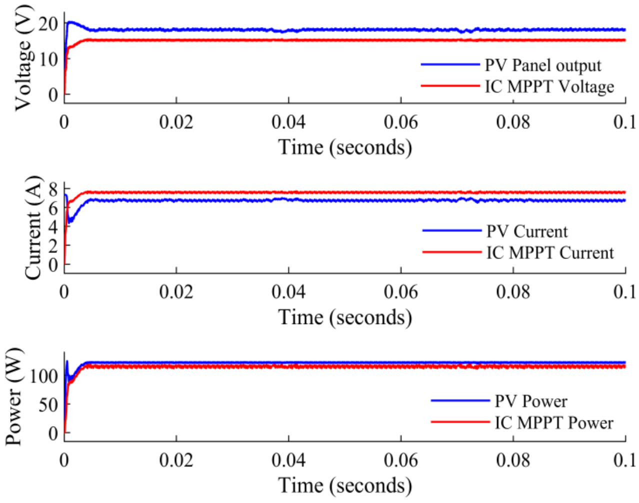


Fig 11. Voltage, Current and Power output of IC MPPT for 1000 W/m$^2$ irradiance level at 25$^o$C.

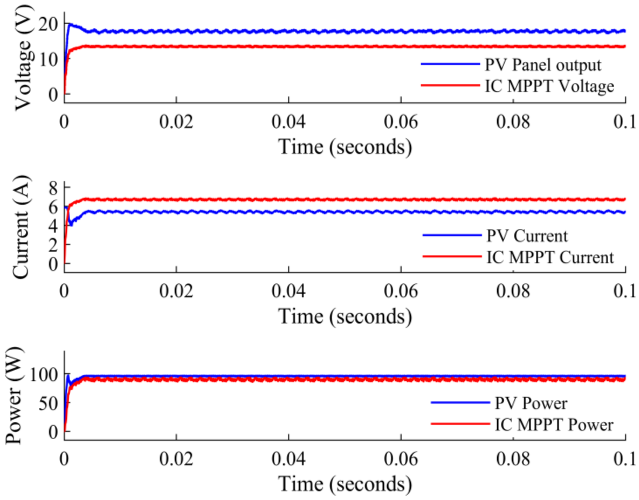


Fig 12. Voltage, Current and Power output of IC MPPT for 800 W/m$^2$ irradiance level at 25$^o$C.

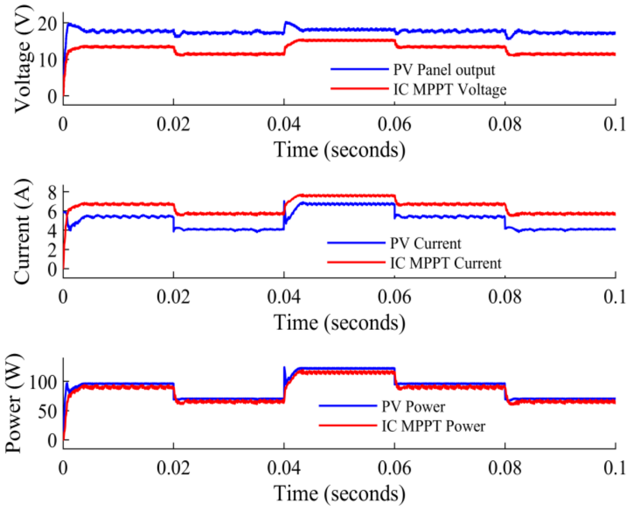


Fig 13. Voltage, Current and Power output of IC MPPT for Step irradiance at 25$^o$C.

Figures 11, 12 and 13 shows the simulation output of IC MPPT, from these Figures it can be clearly seen that, IC tracking is better than P&O MPPT, but output still consists of oscillations in all three cases of irradiance.

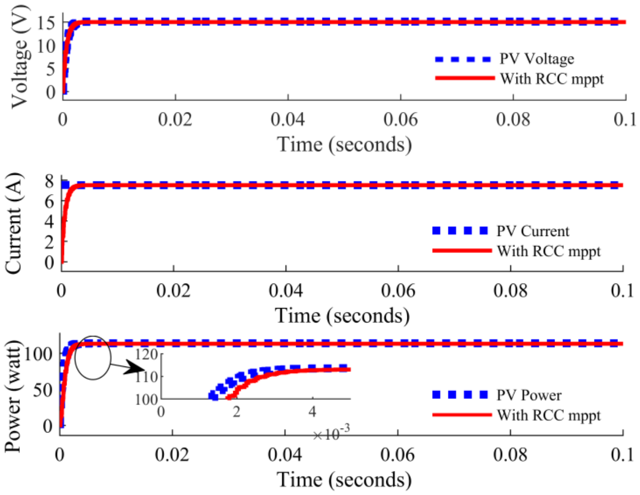


Fig 14. Voltage, Current and Power output of RCC MPPT for 1000 W/m$^2$ irradiance level at 25$^o$C.

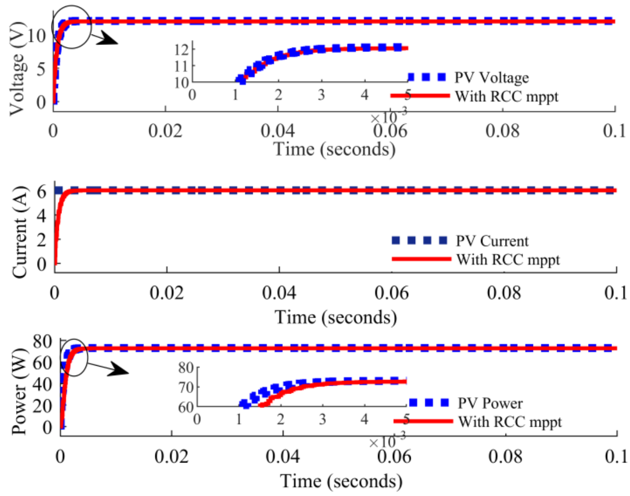


Fig 15. Voltage, Current and Power output of RCC MPPT for 800 W/m$^2$ irradiance level at 25$^o$C.

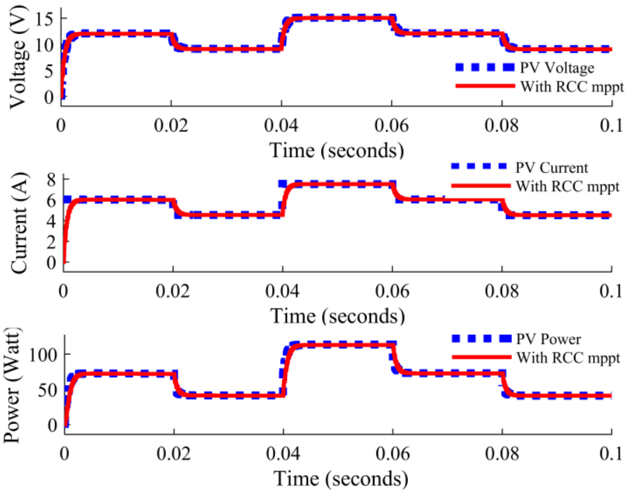


Fig 16. Voltage, Current and Power output of RCC MPPT for Step irradiance at 25$^o$C.

From the Figures 14-16, it can be clearly seen that the problem of slow tracking and ripples (oscillations) has been solved by RCC MPPT. Simulation results verify that RCC MPPT is capable of solving both these problems effectively. Basically these ripples were internal, generated due to use of power electronic converters, and RCC utilizes these internal

Copyright © AJSE Publishers

ripples as perturbations, and is able to eliminate them. Ripple problem is completely solved by RCC MPPT, but for tracking problem can be further improved by some adaptive control strategies.

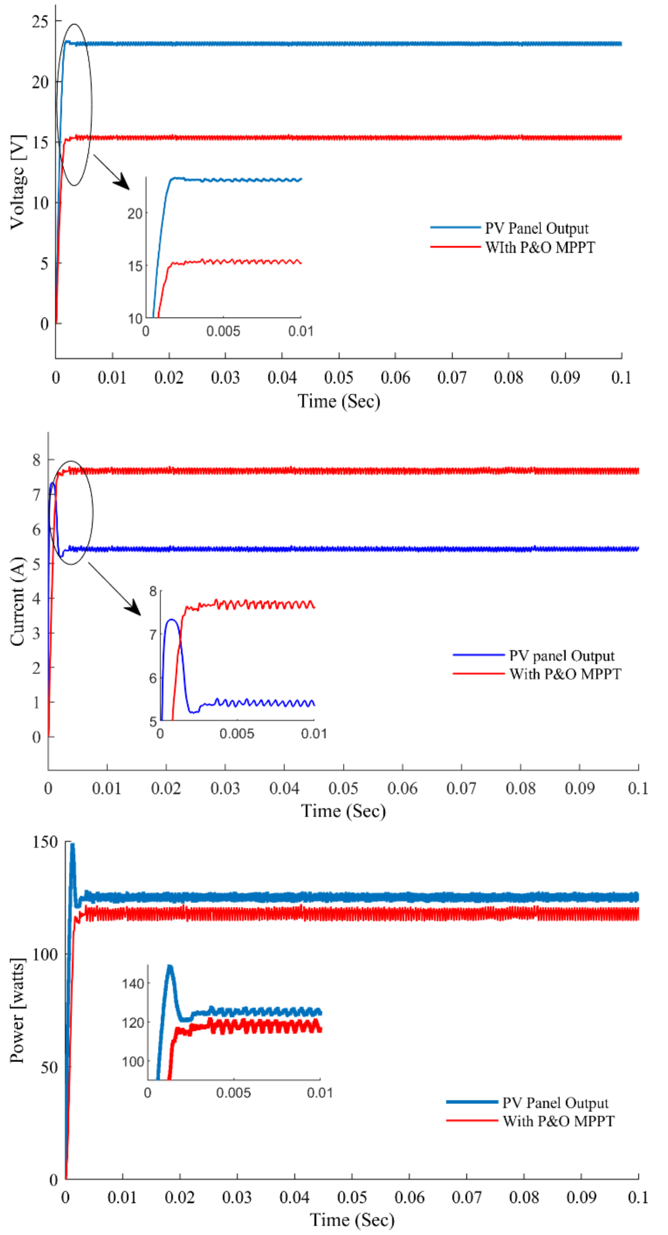


Fig 17. Voltage, Current and Power output of P&O MPPT for 1000 W/m$^2$ irradiance level at 70$^o$C.

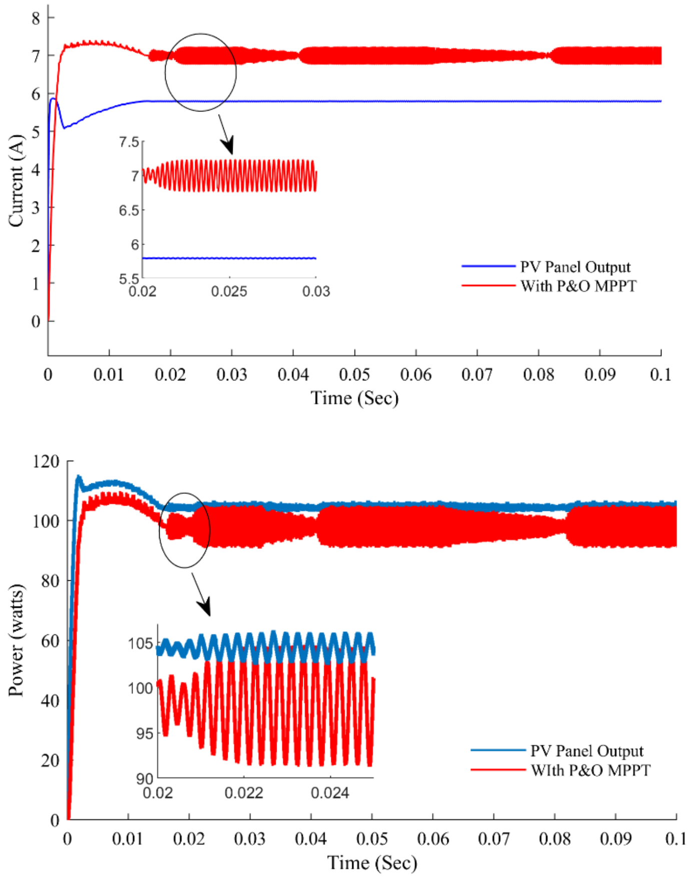


Fig 18. Voltage, Current and Power output of P&O MPPT for 800 W/m$^2$ irradiance level at 70$^o$C.

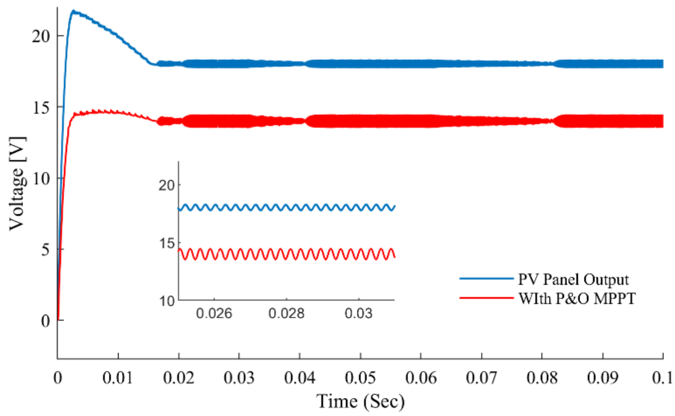


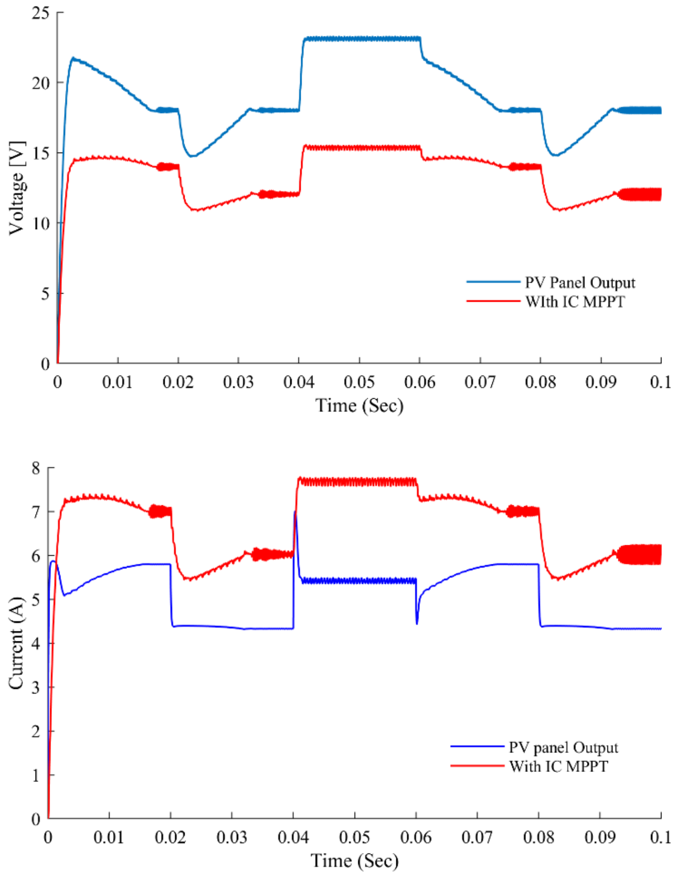

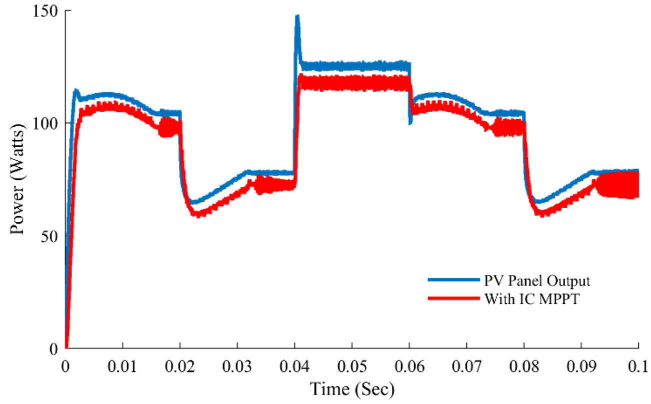


Fig 19. Voltage, Current and Power output of P&O MPPT for Step irradiance at 70°C.

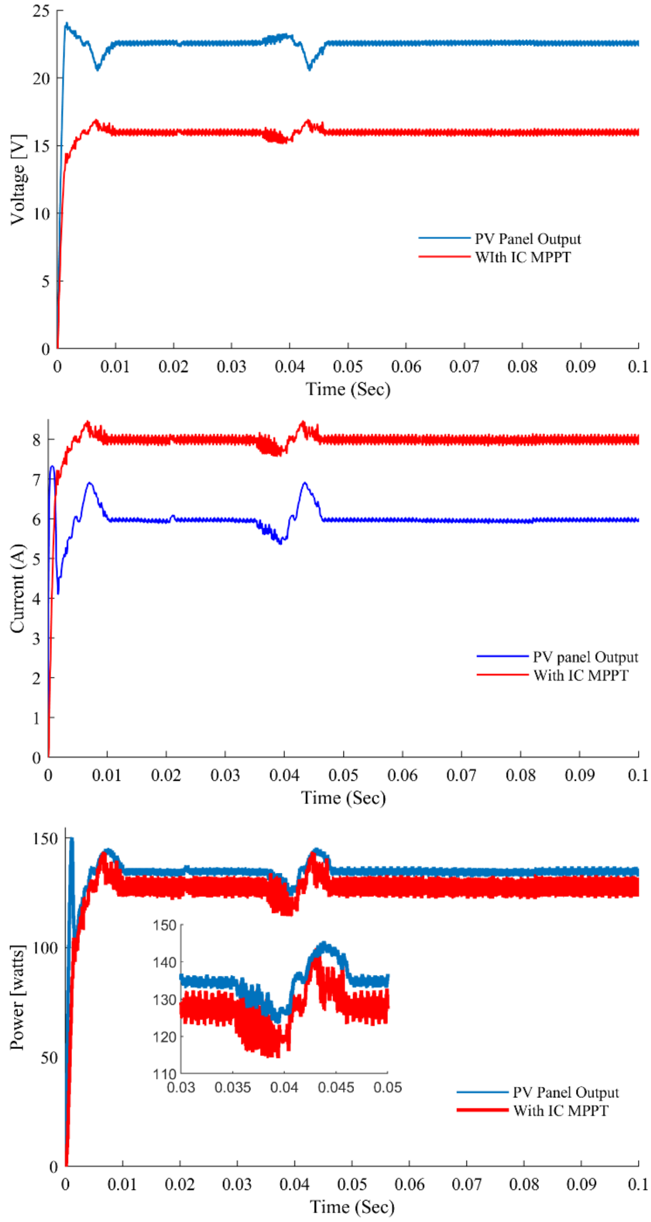


Fig 20. Voltage, Current and Power output of IC MPPT for 1000 W/m$^2$ irradiance level at 70°C.

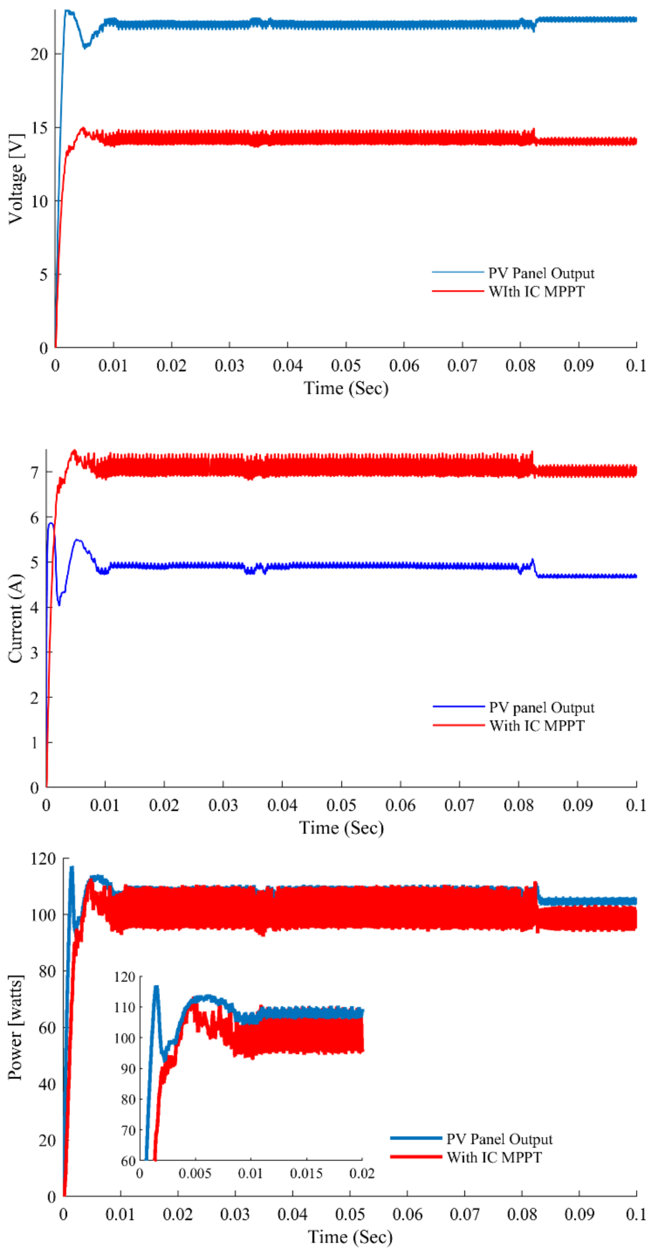


Fig 21. Voltage, Current and Power output of IC MPPT for 800 W/m$^2$ irradiance level at 70°C.

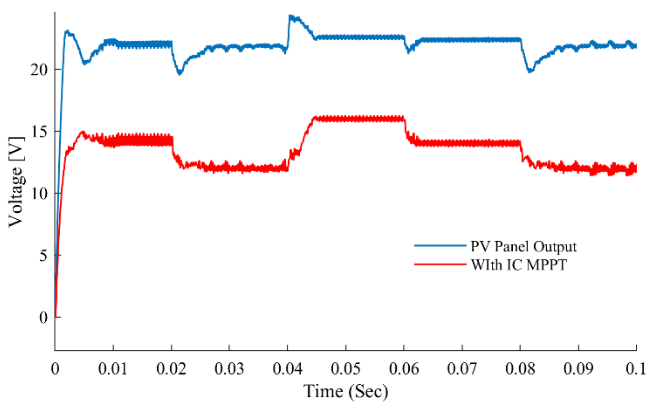

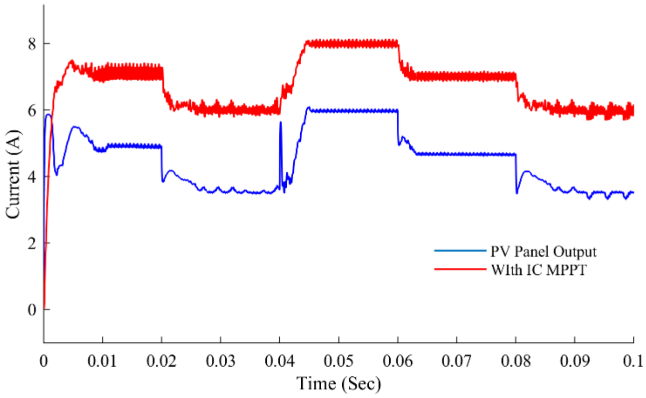


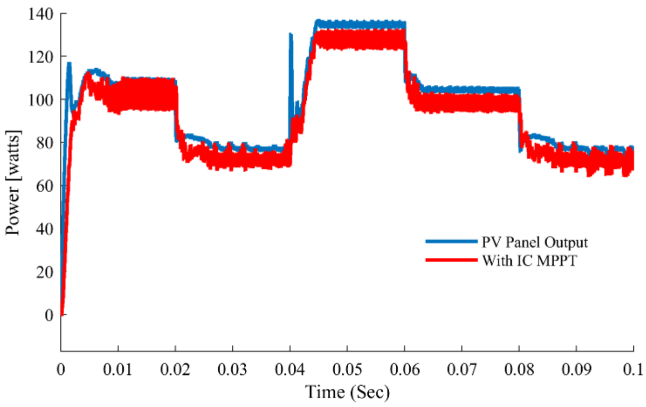


Fig 22. Voltage, Current and Power output of IC MPPT for Step irradiance at 70°C.

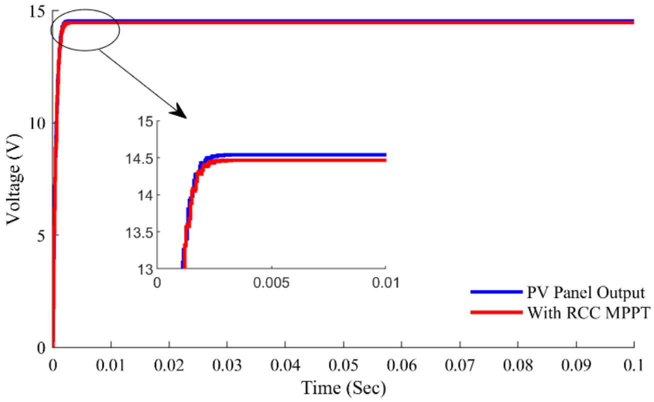


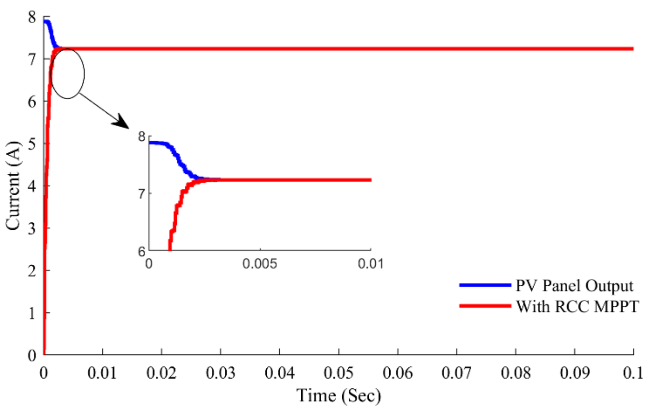


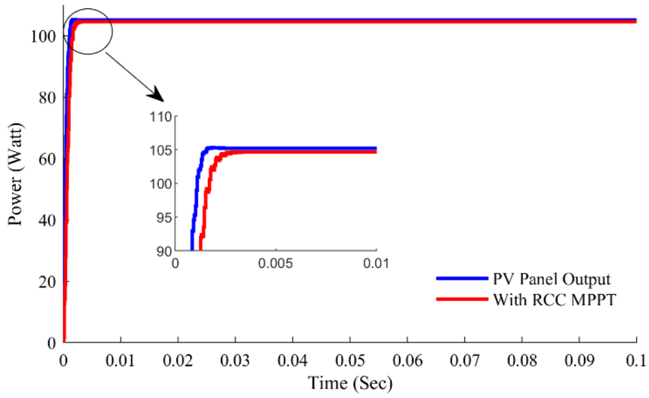


Fig 23. Voltage, Current and Power output of RCC MPPT for 1000 W/m$^2$ irradiance level at 70°C.

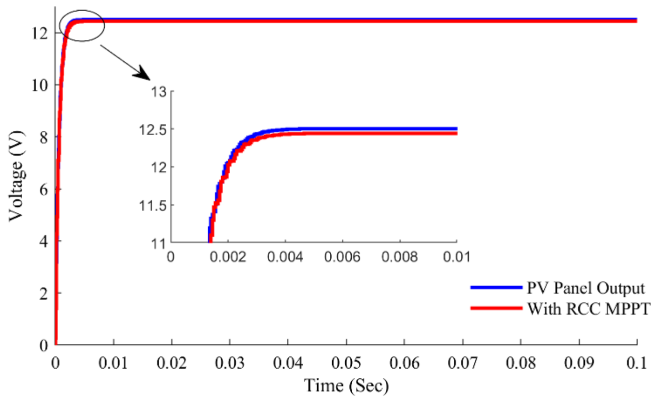


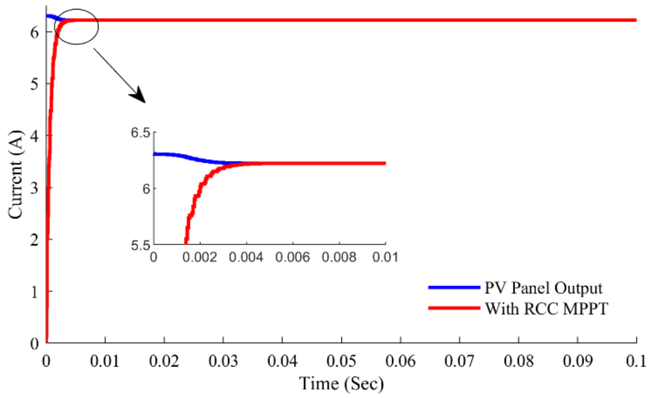


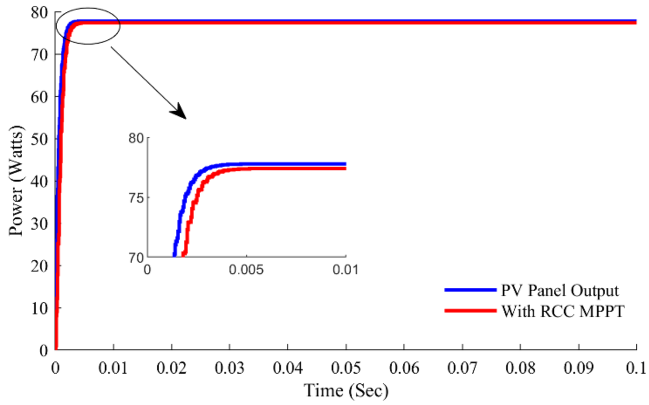


Fig 24. Voltage, Current and Power output of RCC MPPT for 800 W/m$^2$ irradiance level at 70°C.

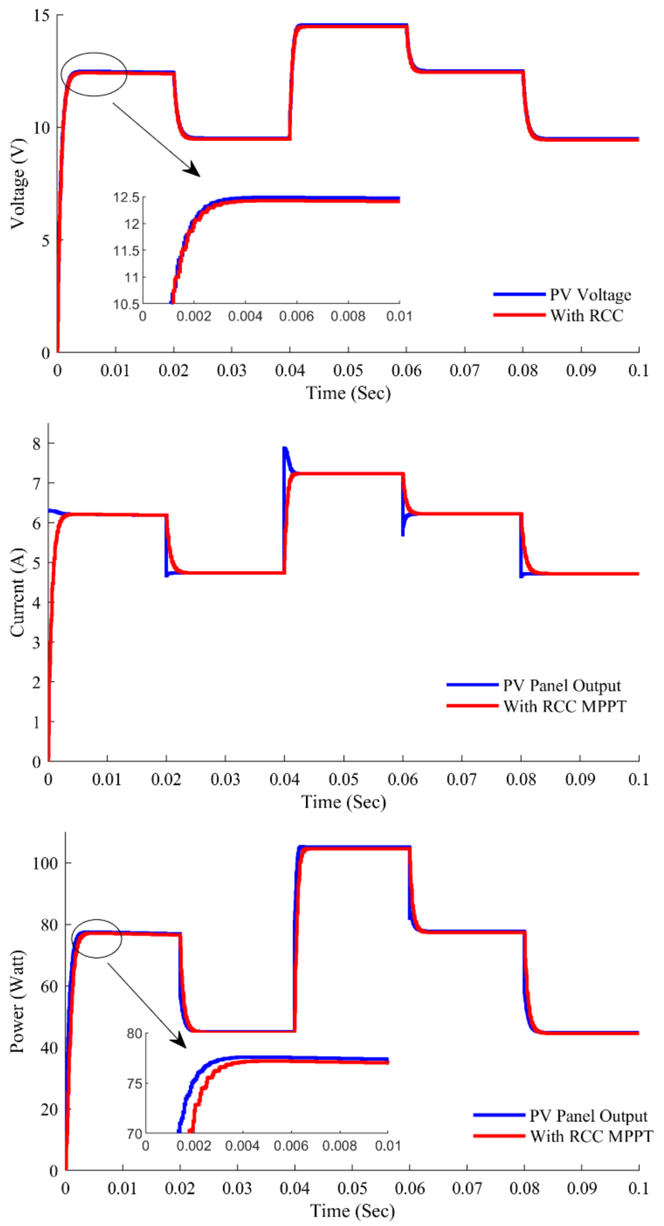


Fig 25. Voltage, Current and Power output of RCC MPPT for Step irradiance at 70ºC.

From the Figures 23-25, it can be clearly seen that the problem of slow tracking and ripples (oscillations) has been solved by RCC MPPT as it performs at lower temperatures. Simulation results verify that RCC MPPT is capable of solving both these problems effectively. Basically, these ripples were internal, generated due to use of power electronic converters, and RCC utilizes these internal ripples as perturbations, and is able to eliminate them. Ripple problem is completely solved by RCC MPPT, but for tracking problem can be further improved by some adaptive control strategies.

## V. Conclusion

This paper presents a comparative study between perturb & observe, incremental conductance and ripple correlation control MPPT. The PV system model used for simulation consists of the PV panel, the variant subsystem of irradiance, the buck converter and the variant subsystem of MPPT controller. This comparative analysis aims to show the improved performance of RCC method over conventional MPPT methods like P&O and IC. The simulation results show that both the methods perturb & observe and incremental conductance have oscillations in current output and hence power output in all three case i.e. 1000 w/m$^2$, 800 w/m$^2$ and step irradiance levels; whereas, RCC MPPT does not has any sort of ripples neither in current output, nor in power output, which is a good sign for longer battery life. Simulations have been performed at 25ºC and 70ºC, for all the techniques, from the results we can conclude that due to semiconductor properties of solar cell, the performance at 25ºC is better than 70ºC. Further, RCC performance can be made more improved in terms of tracking, by using a suitable adaptive control strategy. The work can be also extended by more range of temperature in analysis, with the inclusion of more MPPT techniques for comparison, along with hardware implementation.

## REFERENCES

[1] Femia Nicola, Petrone Giovanni, Spagnuolo Giovanni. Optimization of perturb and observe maximum power point tracking method. *IEEE Trans., on Power Electronics* 2005; 20(4). 963–73.

[2] Pandey Ashish, Dasgupta Nivedita, Mukerjee Ashok Kumar. High-performance algorithms for drift avoidance and fast tracking in solar mppt system, *IEEE Trans., on Energy Converters* 2008;23. 681–9.

[3] Abdelsalam Ahmed K, Massoud Ahmed M, Ahmed Shehab, Enjeti Prasad N., High-performance adaptive perturb and observe MPPT technique for photovoltaic-based micro grids. *IEEE Trans., on Power Electronics* 2011; 26(4). 1010–21.

[4] Mohammed A, Elgendy Bashar, Zahawi, Atkinson David J. Assessment of perturb and observe MPPT algorithm implementation techniques for PV pumping applications. *IEEE Trans., on Sustainable Energy* 2012; 3(1). 21–33.

[5] Ioan Viorel Banu et al., "Comparative analysis of the perturb-and-observe and incremental conductance MPPT methods", 8TH *IEEE International Symposium on Advanced Topics in Electrical Engineering (ATEE),* 2013.

[6] Zainuri Muhammad Ammirrul Atiqi Mohd, Radzi Mohd Amran Mohd, Soh Azura Che, Rahim Nasrudin Abd. Development of adaptive perturb and observe-fuzzy control maximum power point tracking for photovoltaic boost dc–dc converter. *IET Renew Power Gener*., 2014;8(2). 183–94.

[7] Kollimalla Sathish Kumar, Mishra Mahesh Kumar. A novel adaptive P&O MPPT algorithm considering sudden changes in the irradiance. *IEEE Trans., on Energy Converters*, 2014; 29(3). 602–10.

[8] Mohammed A Elgendy, Zahawi Bashar, Atkinson David J. Operating characteristics of the P&O algorithm at high perturbation frequencies for standalone PV systems. *IEEE Trans., on Energy Converters*, 2015; 30(1). 189–98.

[9] Ahmed Jubaer, Salam Zainal. "An improved perturb and observe (P&O) maximum power point tracking (MPPT) algorithm for higher efficiency", *Applied Energy* 2015;150. 97–108.

[10] Raedani Ronn Hanif Moin, "Design, testing and comparison of P&O, IC and VSSIR MPPT technique," *In proceedings of the 3rd international conference on renewable energy research and applications*, 2014, p. 19–22.

[11] LeeJae., HoBaeHyunSu., and ChoBo Hyung., "Advanced incremental conductance MPPT algorithm with a variable step size.", *In proceedings of the 12th International power electronics and motion control conference*, 2006. EPEPEMC 2006.

[12] Li Jiyong, Wang Honghua. A novel stand-alone PV generation system based on variable step size INC MPPT and SVPWM control. *IEEE Conf.,PEMC* 2009. 2155–60.

[13] Hsieh Guan-Chyun, Hsieh Hung-I, Tsai Cheng-Yuan, Wang Chi-Hao. Photovoltaic power-increment-aided incremental-conductance MPPT with two phased tracking. *IEEE Trans Power Electr.,* 2013;28(6). 2895–911.

[14] Uma Maheswara Bala Murali, Rao Ch V.Krishna, Srihari Babu A, Suman S. Design and simulation of PV system with incremental conductance method for maximum power point tracking. *International Journal of Scientific Engineering and Technology* (ISSN. 2277-1581); 3(5). 2014. p. 643-46.

[15] Sivakumar P, Kader Abdullah Abdul, Kaliavaradhan Yogeshraj, Arutchelvi M. Analysis and enhancement of PV efficiency with incremental conductance MPPT technique under non-linear loading conditions, *Renew., Energy* 2015; 81. 543–50.

[16] Veerachary M, Senjyu T, Uezato K. Maximum power point tracking control of IDB converter supplied PV system. *IEEE Proceeding on Electronics Power Applications* 2001. 494–502.

[17] Weidong X, Dunford WG. A modified adaptive Hill Climbing MPPT method for photovoltaic power systems. *IEEE Power Electron Spec Conference*, 2004;35. 1957–63.

[18] Liu Fangrui, Kang Yong, Zhang Yu and Duan Shanxu. Comparison of P&O and Hill Climbing MPPT Methods for Grid-Connected PV Converter. *In Proceedings of the 3rd IEEE conference on industrial electronics and applications*, ICIEA 2008.

[19] J. Prasanth Ram, T. Sudhakar Babu, N. Rajasekar, Renewable and Sustainable Energy Reviews, *Renewable and Sustainable Energy Reviews* 67 (2017) 826–847.

[20] Mingxuan Mao et al., "Maximum Power Point Tracking for Cascaded PV-Converter Modules Using Two-Stage Particle Swarm Optimization", *Nature Scientific Reports*, Article number. 9381, 2017.

[21] Pallab Midya et al., "Dynamic Maximum Power Point Tracker for Photovoltaic Applications", *IEEE Power Electronics Specialists Conference*, 1996.

[22] Philip T.Krein, "Ripple Correlation Control, With Some Applications", *IEEE International Symposium on Circuits and Systems (ISCAS),* 1999.

[23] Raghav Khanna et al., "Maximum Power Point Tracking Using Model Reference Adaptive Control", *IEEE Trans., on Power Electronics*, 2014.

[24] Alessandro Costabeber et al., "Convergence Analysis and Tuning of a Sliding-Mode Ripple-Correlation MPPT", *IEEE Trans., on Energy Conversion*, 2014.

[25] Satish R et *al*., "A Maximum Power Point Tracking Technique Based on Ripple Correlation Control for Single-Phase Single-Stage Grid Connected Photovoltaic System", Science Direct, *Energy Procedia*, 2016.

[26] Salman Salman, Xin AI* et *al*, Design of a P-&-O algorithm based MPPT charge controller for a stand-alone 200W PV system, Springer Protection and Control of Modern Power Systems, 2018.

[27] Pankaj Sahu et *al*., "Ripple Correlation Control Maximum Power Point Tracking for Battery Operated PV Systems: A Comparative analysis," 2020 IEEE International IOT, Electronics and Mechatronics Conference (IEMTRONICS), Vancouver, BC, Canada, 2020, pp. 1-6, doi: 10.1109/IEMTRONICS51293.2020.9216414.

# A Novel Idea of Imagine & Real Speech Decoding Model Using Electrocardiogram to Enhance BCI

Chowdhury S. Islam

***Abstract*— Many researchers have tried to decode talked and guessed speech instantly from brain signals towards the growth of a raw-speech BCI. This paper intends to feature extraction and decoding, using the electrocorticoscope (ECoG), the auditory and articulatory features of the motor cortex. Consonants were selected as auditory depictions, and both positions of articulation and manners of articulation were selected as articulatory depictions. The auditory and articulatory representations were decoded at different time lags concerning the speech onset to find optimal temporal decoding parameters. Moreover, this work explores the role of the temporal lobe during speech production directly from ECoG signals. Also, their temporal propagation before and after the speech onset was performed using classification and statistical tests. A novel decoding model using temporal lobe activity was developed to predict a spectral representation of the speech envelope during speech production. Deep learning was utilized in our analysis. This new knowledge may be used to enhance existing speech-based BCI systems, which will offer a more natural communication modality. Also, the work contributes to the field of speech neurophysiology by providing a better understanding of speech processes in the brain.**

***Keywords*— *electrocorticogram; EEG; fMRI; deep learning; BCI;***

## I. Introduction

The main intention of this research is that it specifies the purpose of the temporal lobe through speech construction. Although the role of the temporal lobe is known during speech perception (especially, the auditory cortex), its role during speech production is still not well-defined. Discovering the role of the temporal lobe while speech production takes place can increase the amount of information that is obtained during speech production, which will increase the efficiency of a speech-based BCI system [1]. These analyses highlight the temporal propagation of articulatory and auditory features with respect to the onset at a high temporal resolution. Previous researchers have not used ECoG in such a way [2]. Instead, there were attempts to understand the temporal differences between each representation using fMRI [3] which has a poor temporal resolution. Secondly, these analyses highlight the role of the temporal lobe during speech production as well as the activation/engagement of the temporal lobe along different time lags with respect to speech onset [4]. A very recent fMRI study indicated that there is predictive coding in the auditory cortex during speech production. In our research confirms this conclusion. Lastly, these analyses highlight the usefulness of deep learning [5,6] as an analysis tool in BCI. These collective findings provide important insights toward developing an efficient speech-based BCI system.

## II. Temporal Propagation Characterizing Results

Different sets of words were presented for each subject, and any class that has less than 15 instances is excluded to avoid bias, the number of classes for each subject varies. After excluding rare classes, the number of classes and electrodes for each subject is shown in Table 3.

Table 3 : Subjects classes. M. of A stands for manners of articulation and P. of A stands for places of articulation.

| Subject | Consonants classes number | M. of A classes | P.of A classes | Electrodes number |
|---|---|---|---|---|
| Subject A | 11 | 5 | 3 | 31 |
| Subject B | 13 | 5 | 3 | 9 |
| Subject C | 13 | 5 | 3 | 21 |

The classification indexes curves are based on 2 different window lengths: 300 ms and 600 ms. The analysis started with a time interval, starting from 500 ms prior to the onset for both 300 and 600 ms windows, and ending at 100 ms or 450 ms after the onset in case of 300 ms and 600 ms windows, respectively. Herein, timings before speech onset will be indicated as negative. The places of articulation classification indexes curve based on a 300 ms window length is depicted in Fig. 1b, which indicates a significant positive gain in the performance in the interval [-.35,.05]s which can be described as the interval where the speech production stage is active. The gradual increase and decrease of the classification indexes curve show the consistency of the temporal propagation for this representation. However, for both consonants and manners of articulation classification indexes in Fig. 1a and Fig. 1c respectively, there are two peaks. The first and the second one occur in the intervals [-450,-150] and [-300, 0] respectively for both representations. This can be interpreted by the window length that was chosen (300 ms), which is too short to capture the information related to these two representations. In order to validate the 300 ms-based analysis as well as to test the effect of the window's length, the analysis was repeated with the 600 ms window's length, which is the same window length of the classification analysis. Since the classification results were statistically significant using this window's length, it is reasonable to speculate a higher classification index, at least in the [-300,300] interval. Fig. 2 depicts that classification indexes were improved as it was speculated. These points to the prolonged-time window of neural activity which is needed to capture the features. The consonants representation's maximum classification index was found in the interval [-200,400] which is depicted in Fig. 2a. For the places of articulation which is depicted in Fig. 2b, the classification indexes reached their maximum in the time intervals [-300,300]. In case of the manners of articulation, the peak of classification index is around [-150,450], where an increase occurs as the window goes to the speech perception

Copyright © AJSE Publishers

stage. Nevertheless, the values of the classification indexes for manners of articulation are very small compared to the other two representations.

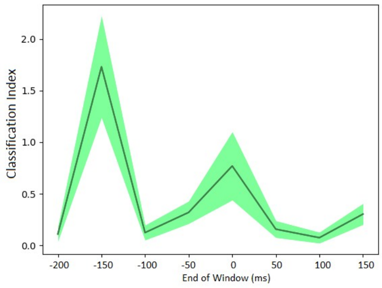


(a) Consonants Classification Indexes

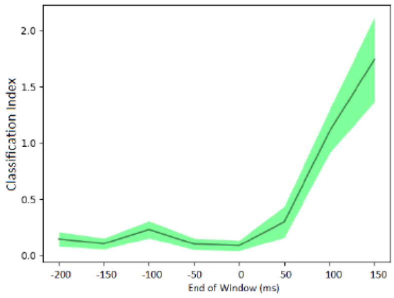


(b) Places of articulation Classification Indexes

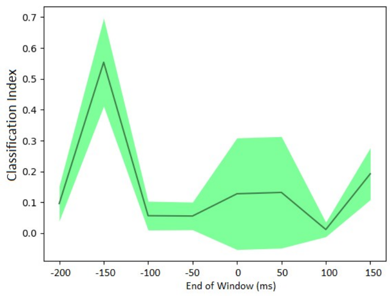


(c) Manners of Articulation Classification Indexes

Fig. 1. The estimated mean of the classification indexes for all articulatory and auditory features of subject A using 300 ms window's length. The shaded area represents the 96% confidence interval.

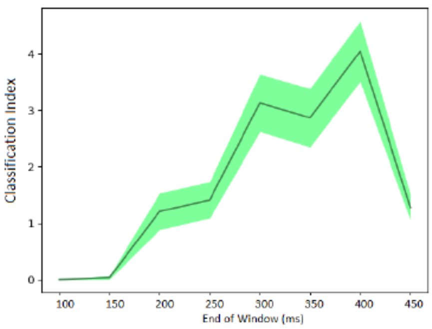


(a) Consonants Classification Indexes

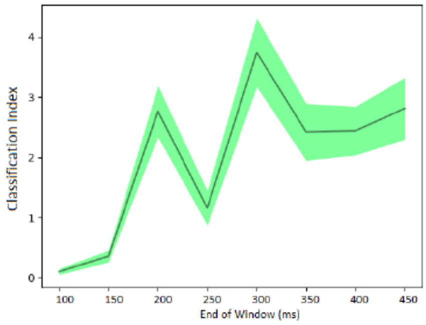


(b) Places of articulation Classification Indexes

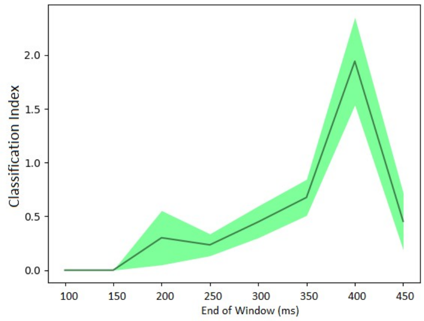


(c) Manners of Articulation Classification Indexes

Fig. 2. The estimated mean of the classification indexes for all articulatory and auditory features of subject A using 600 ms window. The area of shaded stands for the 96% assurance interval. The X-axis depicts the shift by 50 ms of the features window. The Y-axis represents the classification index.

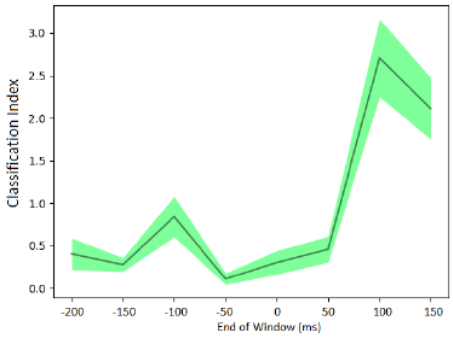


(a) Consonants Classification Indexes

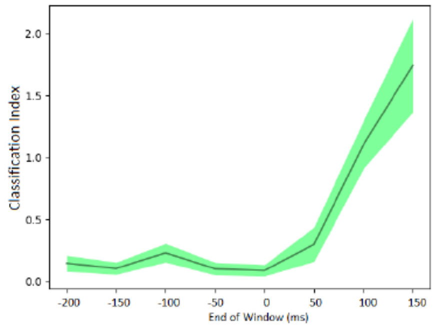


(b) Places of articulation Classification Indexes

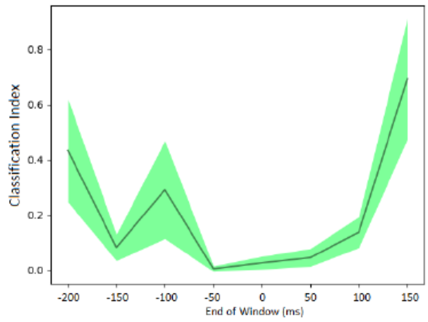


(c) Manners of Articulation Classification Indexes

Fig. 3. The estimated mean of the classification Indexes for all articulatory and auditory features of subject C using 300 ms window. The area of shaded depicts the 96% confidence interval. The X-axis depicts the shift by 50 ms of the features window. The Y-axis represents the classification index

On the other hand, when increasing the window's length to 600 ms, depicted in Fig. 4c, the performance was enhanced and reached its maximum in the interval [-400,200], then decreased and remained constant with a smooth oscillation. The steady state of the curve (smooth oscillations) indicates that no information is gained or lost by shifting the window farther. The places of articulation classification indexes based on the 300 ms window's length are depicted in Fig. 3b, which depicts an increase in the classification indexes all along the interval of [-300,1500] and the maximum classification index occurred in the interval [-150,150]. When increasing the window's length to 600 ms, the places of articulation classification indexes curve did not change as is depicted in Fig. 4b. The consonants classification indexes based on 300 ms window's length is depicted in Fig. 3a. This curve depicts no significant classification index except in the interval [-150,150]. Nonetheless, after increasing the window's length to 600 ms, the consonants classification indexes curve, which is depicted in Fig. 4a, depicts a high classification index in the interval [-300,300] and the performance remains merely constant up to the interval [-100,400], which indicates that no information is gained or lost when shifting the window from [-300,300] to [-100,400]. The analysis of the subject B based on the 300 ms window's length is depicted in Fig. 5. Consonants classification index based on the 300 ms window's length curve in Fig. 5a is maximized during the interval [-150,150] which is the closest interval to speech perception. The manners of articulation classification indexes based on the 300 ms window's length curve is depicted in Fig. 5c, which has a behavior similar to the consonants curve, where it is maximized in the interval [-150,150]. However, the values of

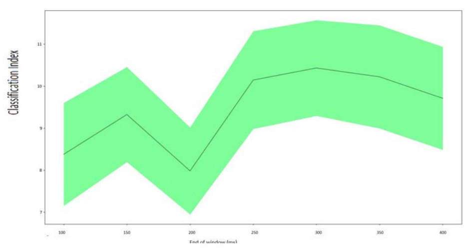


(a) Consonants Classification Indexes

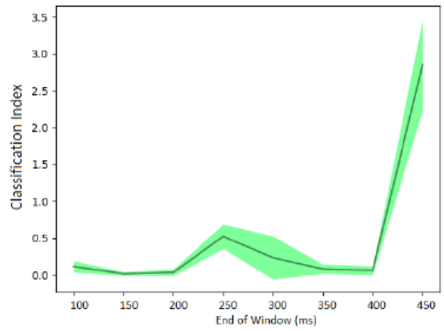


(b) Places of articulation Classification Indexes

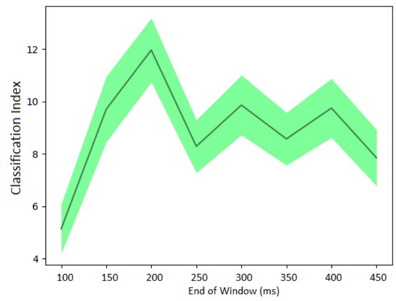


(c) Manners of Articulation Classification Indexes

Fig. 4. The estimated mean of the classification indexes for all articulatory and auditory features of subject C using 600 ms window. The area of shaded depicts the 96% interval of confidence. The X-axis depicts the shift by 50 ms of the features window. The Y-axis represents the classification index.

manners of articulation classification indexes are much less than consonants. Places of articulation classification indexes based on the 300 ms window's length curve is depicted in Fig 11b, where it starts to increase in the interval [-400,-100] up to the interval [-200,100] which includes a speech-perception related activity. To further investigate the effect of the speech-perception stage, the analysis was extended to the 600 ms window's length which is depicted in Fig. 6. The manners of articulation classification indexes curve is depicted in Fig. 5c, where it is maximized in the interval [-250,350]. The places of articulation classification indexes curve, which is depicted in Fig. 6b, has a consistent increase starting from the interval of [-500, 100] and then it is maximized in the interval [-.3,.3], and after that, the curve starts to decrease. The consonants classification indexes curve is depicted in Fig. 6a, which has a consistent increase starting from [-500,100] and then it is maximized in the interval [-250,350], then it is followed by a decrease. The decrease of both consonants and places of articulation curves tells that shifting the window farther after the classification index-maximized interval causes loss of information. Based on the extended analysis of each subject, the temporal characterization of the auditory features, which are represented by consonants, based on the 300 ms window length depicts a higher classification index as temporal-parameters of the features go toward the speech perception stage. Furthermore, the temporal characterization based on the 600 ms window length supports this conclusion, that the speech-perception stage is more related to auditory features than speech-production. Neither of the articulatory features

Copyright © AJSE Publishers

representations, however, depicts consistent temporal classification indexes across subjects for both representations. For instance, subject B showed high manners of articulation temporal classification indexes but also showed weak temporal classification indexes for the places of articulation. In general, the articulatory features and auditory features show higher classification indexes in the case of the 600 ms window's length compared to the 300 ms window's length. In other words, both representations are distributed in a prolonged-time window and they are represented in a time interval larger than 300 ms. Nevertheless, the 600 ms window seems to be too long since the curves usually showed a steady-state classification index when shifting the window farther, for instance, subject C consonants (10c) and manners of articulation ( 10a) classification indexes curves, in addition to

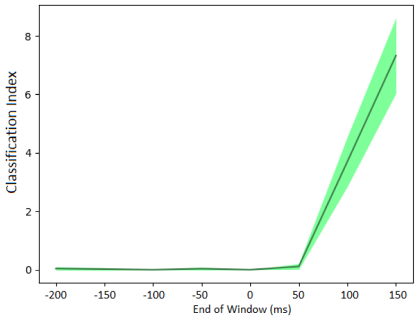


(a) Consonants Classification Indexes

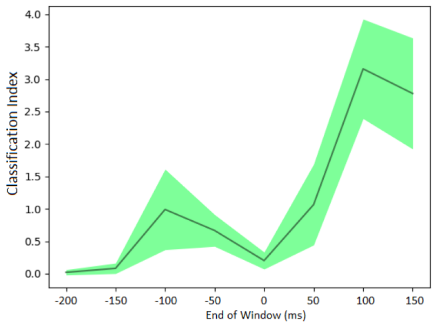


(b) Places of articulation Classification Indexes

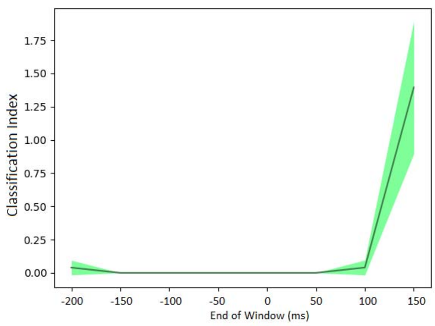


(c) Manners of Articulation Classification Indexes

Fig. 5. The estimated mean of the activation Indexes for all articulatory and auditory features of subject B using 300 ms window. The area of shaded depicts the 96% interval of confidence. The X-axis depicts the shift by 50 ms of the features window. The Y-axis represents the activation index.

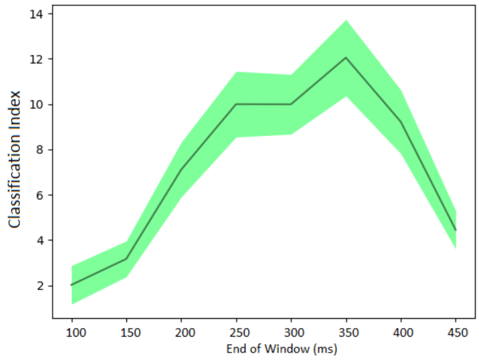


(a) Consonants Classification Indexes

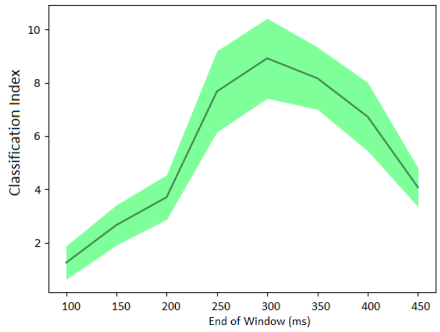


(b) Places of articulation Classification Indexes

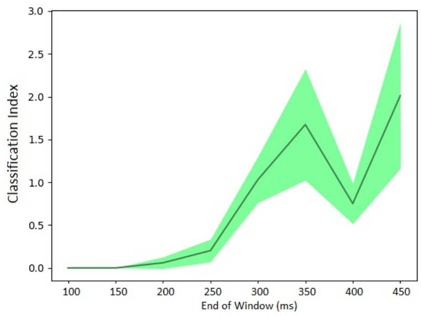


(c) Manners of Articulation Classification Indexes

Fig. 6. The estimated mean of the classification Indexes for all articulatory and auditory features of subject B using 600 ms window. The area of shaded depicts the 96% interval of confidence. The X-axis depicts the shift by 50 ms of the features window. The Y-axis represents the classification index.

subject A places of articulation classification indexes curve ( 8b). Further analysis must be done to capture the best window length for each representation.

In general, the temporal characterization of the auditory features has a more consistent classification indexes curve. On the other hand, the temporal characterization of the articulatory features, which are represented by place and manners articulations, varied across subjects. More specifically, subjects A and C have consistent classification indexes for the places of articulation, but subject B has more consistent classification indexes for the manners of articulation. Fig. 7 depicts the typical and standard deviation of all representations across the three subjects. The Consonants curve, depicted in Fig. 7a depicts that the

Copyright © AJSE Publishers

classification indexes increase as the time window is shifted toward speech perception. Places and manners of articulation show a high standard deviation since the classification indexes for these two representations significantly varied across subjects. However, since places of articulation were better represented for two subjects and manners of articulation were better represented for a single subject, the standard deviation of the places of articulation is less than the standard deviation of manners of articulation across subjects.

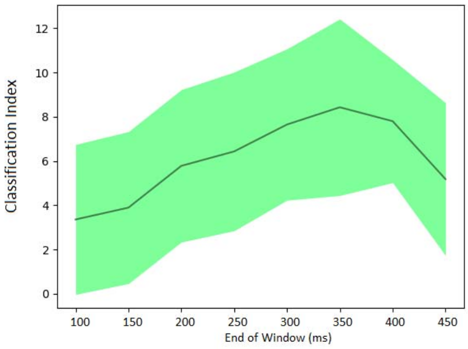


(a) Average and Standard Deviation of Consonants Classification Indexes across Subjects

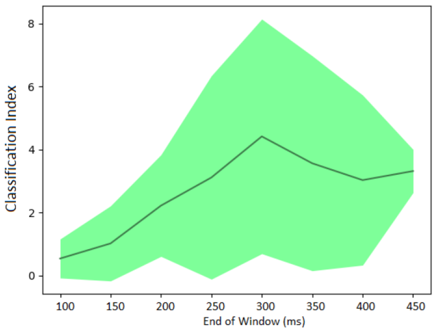


(b) Average and Standard Deviation of Places of Articulation Classification Indexes across Subjects

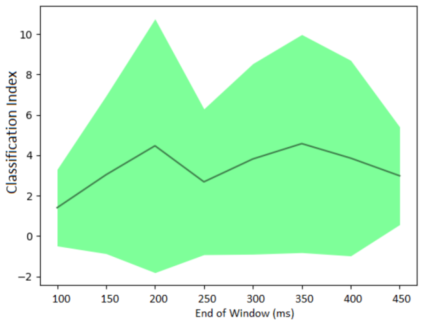


(c) Average and Standard Deviation of Manners of Articulation Classification Indexes across subjects

Fig. 7. The estimated mean of the classification Indexes for all articulatory and auditory features of subject B using 600 ms window. The area of shaded depicts the 96% interval of confidence. The X-axis depicts the shift by 50 ms of the features window. The Y-axis represents the classification index.

## III. Modeling speech-related neural activities in the temporal lobe

Most of the selected electrodes of subject A were located at the inferior part of the temporal lobe, which is distant from the auditory cortex. Subject D has the best coverage of the temporal lobe, especially the auditory cortex. The critical value $\alpha_{.05}$ of the chance level Pearson correlation coefficient was estimated in order to have a simple and easy way to read results. The $\alpha_{.05}$ of the chance level Pearson correlation coefficient was calculated for each shift, subject, and frequency group. That is, $4 \times 11 \times 7$ different critical values were obtained, where the 1st number refers to the number of subjects, the 2nd refers to the number of shifts, and the 3rd refers to the number of frequencies group. In order to understand how these critical values differ according to their parameters (i.e., subjects, frequency groups, and lags), they were grouped based on their shift. For instance, all critical values of -500 ms lag were best-fitted to a distribution. It was found that all shift-based groups followed a Normal distribution with very close means [.7,.10]. This means that the distributions of these grouped critical values are merely the same. Therefore, all critical values were bestfitted to a distribution, and it was found that they followed a Gaussian distribution with a mean of .09. This means that different parameters (i.e., subjects, frequency groups, and lags) do not affect the values of α.05.

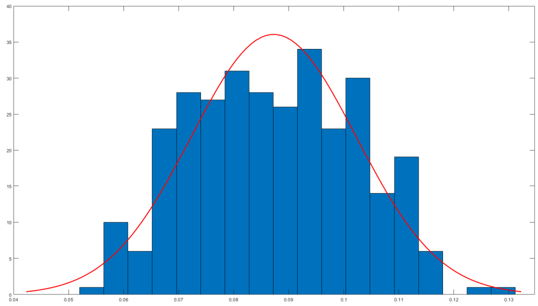

Fig. 8. The critical values obtained from different shifts, frequency groups, and subjects.

This calculation yields $\alpha_{.05}$ = .0.1156, which would be considered one of the largest extreme values that a level of chance correlation could take which depicts in Fig. 8.

Fig. 9 depicts the mean, which is represented by the black curve, and the standard deviation, which is represented by the gray shaded area, of the correlation coefficients over different lags across the 4 subjects. The lowest frequency group [1-3]Hz starts from the top, and the higher frequency group [19-21]Hz ends down at the bottom. The x-axis represents the lags starting from -500 ms and up to 500 ms (11 shifts). The red horizontal line represents the critical value α.05 of the level of chance. Based on Fig. 9, which depicts the Pearson correlation coefficients from -500 ms to 500 ms lags with 100 ms increase, the propagation curves start to increase from -.5 s to a point in the interval [.1,.2] s and then start to decrease where speech-related activity starts to diminish.

Copyright © AJSE Publishers

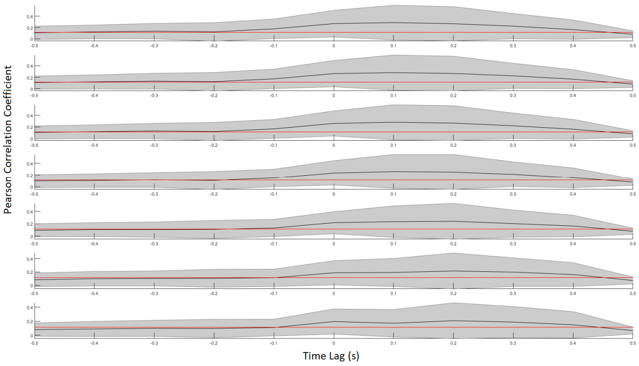


Fig. 9. The Mean and standard deviation of the average correlation coefficient across the 4 subjects for each frequency group between predicted and the actual output of the testing data.

Fig. 10 depicts the Pearson correlation coefficients of subject D. Each curve represents a frequency group. The analysis starts at 500 ms before the onset and ends at 500 ms after the onset with an increase of 100 ms. All values in Matlab on the curve are statistically significant above the level of chance ($p \leq .001$) except when speech leads ECoG signals by 500 ms (i.e., the last point on the curve). For instance, the first group ($f_1$ in Fig. 1), which is the mean of values at the integer frequencies power in the interval [1-3], has the best correlation with the actual signal and the second higher correlation is assigned to the second group of frequencies [4-6] and so on.

This analysis depicts that there is stronger speech-related neural activity in the very early stage of speech production (-500 ms prior) whereas the previous analysis showed there is either no or very weak speech-related activity in the temporal lobe before -220 ms with respect to the speech onset. It can be interpreted by the LSTM-RNN model is able to capture the nonlinear correlations between the ECoG and speech signals since the prior work was based on Pearson correlation coefficients between speech and neural activities. The performance of the linear regression along with the performance of the LSTM-RNN model is depicted in Fig. 11. For time lags -200 ms prior, the linear model depicts much

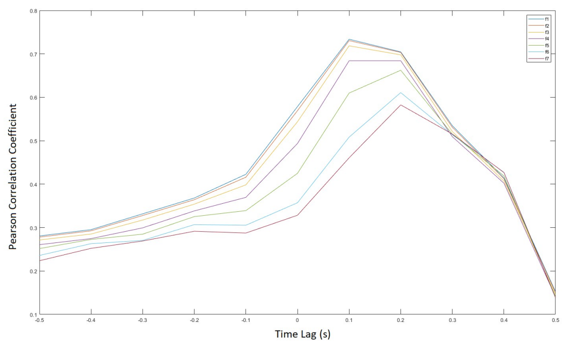


Fig. 10. Decoding the frequencies of speech envelope from subject D temporal lobe using the gamma envelope based on LSTM-RNN model.

weaker correlation coefficients compared with LSTM-RNN model. This may indicate the

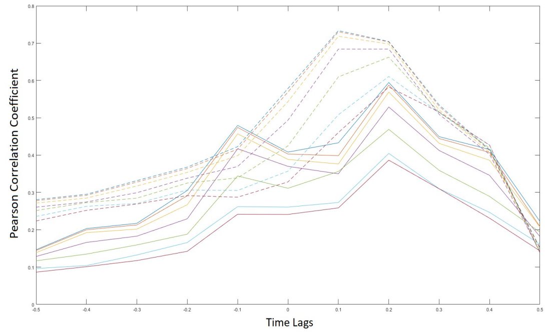


Fig. 11. Linear Model Performance (solid lines) VS LSTM-RNN (dashed lines) performance.

nonlinear relationship between the neural activity in the temporal lobe in the very early the speech production stage and the speech activity. Fig. 11 also depicts the better performance of LSTM-RNN over the linear model [7, 8]. Another interpretation is that, in this work, the spectral power of the speech envelope provides a better representation than the raw envelope used in the prior study.

## IV. Conclusion

The two main results of the speech-based BCI indicate that, firstly, the articulatory features appear before the auditory features in the motor cortex by 50 to 150 ms, and auditory features are most relevant to the speech perception stage. Secondly, the temporal lobe is able to predict speech information in the production stage. These two results suggest that multiple decisions can be taken from different regions across different time intervals. Combining these decisions will improve the reliability of the BCI system. For instance, a speech-based BCI can detect the articulatory features from the motor cortex and auditory features from the temporal lobe at the very early stage of speech production. After that, the auditory features are detected from both the motor cortex and the temporal lobe in the late speech production and speech perception stage. Finally, these decisions are combined together to reduce the error and maximize the probability that a detection is correct since more knowledge minimizes the error of machine learning models. This means that a speech-based BCI system can be composed of multiple modules, where each one works on a specific feature representation (e.g., articulatory and auditory) from a specific brain region and at a specific time interval. In other words, each module is specialized in the representation-spatial-temporal decoding technique. Such implementation would lead to improving the real-time speech-based BCI system in a way that if the decision in the early production stage is very confident (i.e., probability of error is too low) then this will help to reduce the response time (i.e., time required to issue a command). This paper contributes to giving possible prototypes of such modules. Another possible usage is that if a speech-based BCI system is mainly implemented to decode the auditory features (e.g., phonemes), an articulatory features-based BCI system can provide support when the former system is confused, in a way that opposes or supports the decision of the auditory features-based system.

Copyright © AJSE Publishers

## REFERENCES


[1] Rashid, M., Sulaiman, N., PP Abdul Majeed, A., Musa, R.M., Ab Nasir, A.F., Bari, B.S. and Khatun, S., 2020. Current Status, Challenges, and Possible Solutions of EEG-Based Brain-Computer Interface: A Comprehensive Review. Frontiers in Neurorobotics.

[2] Okada, K., Matchin, W. and Hickok, G., 2018. Neural evidence for predictive coding in auditory cortex during speech production. Psychonomic bulletin & review, 25(1), pp.423-430.

[3] Berezutskaya, J., Freudenburg, Z.V., Güçlü, U., van Gerven, M.A. and Ramsey, N.F., 2017. Neural tuning to low-level features of speech throughout the perisylvian cortex. Journal of Neuroscience, 37(33), pp.7906-7920.

[4] Conant, D.F., Bouchard, K.E., Leonard, M.K. and Chang, E.F., 2018. Human sensorimotor cortex control of directly measured vocal tract movements during vowel production. Journal of Neuroscience, 38(12), pp.2955-2966.

[5] Riecke, L., Formisano, E., Sorger, B., Başkent, D. and Gaudrain, E., 2018. Neural entrainment to speech modulates speech intelligibility. *Current Biology*, *28*(2), pp.161-169.

[6] Ullah, A., Anwar, S.M., Bilal, M. and Mehmood, R.M., 2020. Classification of Arrhythmia by Using Deep Learning with 2-D ECG Spectral Image Representation. Remote Sensing, 12(10), p.1685.

[7] Peimankar, A. and Puthusserypady, S., 2020. DENS-ECG: A Deep Learning Approach for ECG Signal Delineation. arXiv preprint arXiv:2005.08689.

[8] Zhao, J., Mao, X. and Chen, L., 2019. Speech emotion recognition using deep 1D & 2D CNN LSTM networks. Biomedical Signal Processing and Control, 47, pp.312-323.


Copyright © AJSE Publishers